

Document downloaded from:

<http://hdl.handle.net/10251/141649>

This paper must be cited as:

Egea, I.; Pineda Chaza, B.J.; Ortiz Atienza, A.; Plasencia, F.; Drevensek, S.; García Sogo, B.; Yuste-Lisbona, F.J.... (02-2). The SICBL10 calcineurin B-like protein ensures plant growth under salt stress by regulating Na<sup>+</sup> and Ca<sup>2+</sup> homeostasis. PLANT PHYSIOLOGY. 176(2):1676-1693. <https://doi.org/10.1104/pp.17.01605>



The final publication is available at

<https://doi.org/10.1104/pp.17.01605>

Copyright American Society of Plant Biologists

Additional Information

1 **Running title:**

2 *SICBL10* ensures plant development under salinity

3

4 **Corresponding author:**

5 Rafael Lozano

6 Departamento de Biología y Geología

7 Edificio CITE II-B

8 Universidad de Almería

9 Carretera de Sacramento s/n

10 04120 Almería, Spain

11 Phone: +34 950 015111

12 Fax: +34 950 015476

13 Email: [rlozano@ual.es](mailto:rlozano@ual.es)

14

15 **Title:**

16 **The SICBL10 calcineurin B-like protein ensures plant growth under salt stress by regulating Na<sup>+</sup> and**  
17 **Ca<sup>2+</sup> homeostasis**

18

19

20 **Author names and affiliations:**

21 Isabel Egea<sup>1,#</sup>, Benito Pineda<sup>2,#</sup>, Ana Ortíz-Atienza<sup>3,#</sup>, Félix A. Plasencia<sup>1</sup>, Stéphanie Drevensek<sup>4</sup>, Begoña

22 García-Sogo<sup>2</sup>, Fernando J. Yuste-Lisbona<sup>3</sup>, Javier Barrero<sup>5</sup>, Alejandro Atarés<sup>2</sup>, Francisco B. Flores<sup>1</sup>, Fredy

23 Barneche<sup>4</sup>, Trinidad Angosto<sup>3</sup>, Carmen Capel<sup>3</sup>, Julio Salinas<sup>5</sup>, Wim Vriezen<sup>6</sup>, Elisabeth Esch<sup>7</sup>, Chris Bowler<sup>4</sup>,

24 Maria C. Bolarín<sup>1</sup>, Vicente Moreno<sup>2</sup>, Rafael Lozano<sup>3</sup>

25

26 <sup>1</sup> Centro de Edafología y Biología Aplicada del Segura, Consejo Superior de Investigaciones Científicas. 30100  
27 Espinardo, Murcia, Spain.

28 <sup>2</sup> Instituto de Biología Molecular y Celular de Plantas (UPV-CSIC), Universidad Politécnica de Valencia. Avda.  
29 de los Naranjos, s/n. 46022 Valencia, Spain.

30 <sup>3</sup> Centro de Investigación en Biotecnología Agroalimentaria (BITAL). Universidad de Almería, 04120 Almería,  
31 Spain.

32 <sup>4</sup> Institut de Biologie de l'École Normale Supérieure, Paris Sciences et Lettres Research University, CNRS  
33 UMR 8197, INSERM U1024. F-75005 Paris, France.

34 <sup>5</sup> Centro de Investigaciones Biológicas, Consejo Superior de Investigaciones Científicas. c/ Ramiro de Maeztu,  
35 9. Madrid, Spain.

36 <sup>6</sup> Bayer Vegetable Seeds, 6083 AB Nunhem, The Netherlands.

37 <sup>7</sup> Hild-Samen GmbH. D-71672 Marbach am Neckar, Germany

38

39 <sup>#</sup> These authors contributed equally to this work.

40

41 **One sentence summary:**

42 Tomato CALCINEURIN B-LIKE PROTEIN 10 (SICBL10) ensures plant growth by regulating proper  
43 distribution of Na<sup>+</sup> and Ca<sup>2+</sup> in the shoot apical meristem and developing organs under salt stress.

44

45 **Author contributions:**

46 I.E., B.P., A.O-A., F.A.P., S.D., B.G-S., F.J.Y-L., C.C. and J.B. performed the experiments; A.A., F.B.F., F.B.  
47 and T.A. collaborated in the design of the experiments and data analyses; J.S., W.V., C.B., M.C.B., V.M. and  
48 R.L. conceived the project and research plans, and supervised the experiments; I.E. and R.L. wrote the article  
49 with contributions of all the authors.

50

51 **Funding information:**

52 This study was supported by grants from the Plant KBBE Program (EUI2009-04074), the Spanish Ministerio de  
53 Economía y Competitividad (AGL2012-40150 and AGL2015-64991-C3-1-R/2-R/3-R), as well as the French  
54 National Research Agency ENDOREPIGEN project. A.O-A. was supported by a PhD fellowship from the  
55 Ministerio de Economía y Competitividad (BIO2009-11484).

56

57 **Corresponding author email:**

58 rlozano@ual.es

59

60 **ABSTRACT**

61 Characterization of a new tomato T-DNA mutant allowed for the isolation of the *CALCINEURIN B-LIKE*  
62 *PROTEIN 10 (SlCBL10)* gene whose lack of function was responsible for the severe alterations observed in the  
63 shoot apex and reproductive organs under salinity conditions. Physiological studies proved that *SlCBL10* gene is  
64 required to maintain a proper low  $\text{Na}^+/\text{Ca}^{2+}$  ratio in growing tissues allowing tomato growth under salt stress.  
65 Expression analysis of the main responsible genes for  $\text{Na}^+$  compartmentalization [i.e. *Na<sup>+</sup>/H<sup>+</sup> EXCHANGERS*  
66 (*LeNHX3* and *LeNHX4*), *SALT OVERLY SENSITIVE (SlSOS1* and *SlSOS2)*, *HIGH-AFFINITY K<sup>+</sup>*  
67 *TRANSPORTER 1;2 (SlHKT1;2)*, *H<sup>+</sup>-pyrophosphatase AVP1 (SlAVP1)* and V-ATPase (*SlVHA-A1*)] supported  
68 a reduced capacity to accumulate  $\text{Na}^+$  in *Slcbl10* mutant leaves, which resulted in a lower uploading of  $\text{Na}^+$   
69 from xylem, allowing the toxic ion to reach apex and flowers. Likewise, the tomato *CATION EXCHANGER 1*  
70 (*SlCAX1*) and *TWO-PORE CHANNEL 1 (SlTPC1)*, key genes for  $\text{Ca}^{2+}$  fluxes to the vacuole, showed abnormal  
71 expression in *Slcbl10* plants indicating an impaired  $\text{Ca}^{2+}$  release from vacuole. Additionally, complementation  
72 assay revealed that *SlCBL10* is a true orthologue of the *Arabidopsis CBL10* gene supporting that the essential  
73 function of CBL10 is conserved in *Arabidopsis* and tomato. Together, the findings obtained in this study  
74 provide new insights into the function of *SlCBL10* in salt stress tolerance. Thus, it is proposed that *SlCBL10*  
75 mediates salt tolerance by regulating  $\text{Na}^+$  and  $\text{Ca}^{2+}$  fluxes in the vacuole, cooperating with the vacuolar cation  
76 channel *SlTPC1* and the two vacuolar  $\text{H}^+$ -pumps, *SlAVP1* and *SlVHA-A1*, which in turn are revealed as potential  
77 targets of *SlCBL10*.

78

79 **Keywords:** Salinity, *Solanum lycopersicum*, CBL10, TPC1 channel, vacuolar  $\text{H}^+$ -pumps,  $\text{Na}^+$  and  $\text{Ca}^{2+}$   
80 homeostasis.

81

## 82 INTRODUCTION

83 The development of crop plants tolerant to abiotic stress is crucial to meet the growing food demand through  
84 sustainable agriculture. Along their life cycle, plants need to balance development and adaptive responses to  
85 unfavourable conditions, salinity being one of the most severe factors limiting the productivity of agricultural  
86 crops (Flowers et al., 2010; Shabala, 2013). Significant advances have been made in the study of genes involved  
87 in salt stress tolerance and ion homeostasis (Maathuis, 2014), especially in the model species *Arabidopsis*  
88 *thaliana*, whereas knowledge about species of agronomic interest such as tomato remains scarce. Salt tolerance  
89 is determined by the ability of the plant to regulate  $\text{Na}^+$  transport rate from the root to the shoot through the  
90 xylem and by the capacity to accumulate  $\text{Na}^+$  ion into the vacuoles of the adult leaves and stem, which allows  
91 the plants to protect young developing tissues from  $\text{Na}^+$  toxicity (Shabala, 2013; Maathuis, 2014).  $\text{Na}^+$  efflux is  
92 mediated by the plasma membrane  $\text{Na}^+/\text{H}^+$  antiporter SALT OVERLY SENSITIVE 1 (SOS1; Hasegawa, 2013),  
93 whereas HIGH-AFFINITY  $\text{K}^+$  TRANSPORTER (HKT) proteins, particularly those belonging to class I  
94 (Platten et al., 2006), are critical determinants of  $\text{Na}^+$  unloading from xylem vessels to other cells in the stele  
95 (Hasegawa, 2013). In tomato, two HKT1-like isoforms have been identified, *SlHKT1;1* and *SlHKT1;2*, which  
96 underlie a major tomato QTL for  $\text{Na}^+/\text{K}^+$  homeostasis (Asins et al., 2013). Mainly, *SlHKT1;2* has been involved  
97 in the regulation of  $\text{Na}^+$  movement from root to shoot through xylem and therefore, in the  $\text{Na}^+$  concentration in  
98 leaves under saline conditions (Almeida et al., 2014; Asins et al., 2015). Compartmentalization in the vacuole of  
99  $\text{Na}^+$  ions is an effective mechanism to avoid the toxic effects of  $\text{Na}^+$  in the cytoplasm (Maathuis, 2014). The  
100 transport of  $\text{Na}^+$  from the cytoplasm into the vacuole occurs via tonoplast  $\text{Na}^+/\text{H}^+$  EXCHANGERS (NHXs).  
101 Four NHX isoforms have been identified in tomato; among them, *LeNHX3* and *LeNHX4* show the strongest  
102 induction upon salinity (Galvez et al., 2012). In addition, *LeNHX3* has been associated with a QTL for  $\text{Na}^+$   
103 concentration in leaves (Villalta et al., 2008). In *Arabidopsis*, the  $\text{Na}^+$  compartmentalization process mediated  
104 by vacuolar  $\text{Na}^+/\text{H}^+$  antiporters is driven by the electrochemical gradient of protons across the tonoplast  
105 generated by the vacuolar  $\text{H}^+$  pumps,  $\text{H}^+$ - pyrophosphatase ( $\text{H}^+$ -PPase) AVP1 and V-ATPase (Maeshima, 2000,  
106 Hasegawa, 2013). Two full-length cDNA clones (*SIVHA-A1* and *SIVHA-A2*) coding for two isoforms of the V-

107 ATPase catalytic subunit (V-ATPases A1 and A2) have been isolated in tomato. In response to salinity, the  
108 abundance of the *SIVHA-A1* transcript in leaves was nearly doubled with respect to control conditions, while  
109 *SIVHA-A2* did not change and was mostly expressed in roots (Bageshwar et al., 2005).

110 Salt tolerance in plants also required a proper balance of  $\text{Ca}^{2+}$  and  $\text{Na}^+$  ions (Manaa et al., 2013). Thus, it has  
111 been well documented that  $\text{Ca}^{2+}$  has a direct inhibitory effect on  $\text{Na}^+$  entry into the cell by decreasing  $\text{Na}^+$  influx  
112 through non-selective cation channels and acting as a counter-cation inside storage organelles (Shabala et al.,  
113 2005). However, a  $\text{Ca}^{2+}$  deficit situation can occur in plants growing under salinity, since the elevated  
114 concentration of  $\text{Na}^+$  hinders  $\text{Ca}^{2+}$  uptake by roots (Zhai et al., 2015). The large central vacuole of a typical  
115 mature cell is by far the largest intracellular  $\text{Ca}^{2+}$  storage in plants, therefore, the mobilization of  $\text{Ca}^{2+}$  vacuolar  
116 reservoirs by the plant in this unfavourable situation is crucial to maintain the growth of young tissues (Bonales-  
117 Alatorre et al. 2013). A steady state level of vacuolar  $\text{Ca}^{2+}$  depends on the balance between active  $\text{Ca}^{2+}$  import  
118 to vacuoles and vacuolar channels mediating  $\text{Ca}^{2+}$ -induced  $\text{Ca}^{2+}$  release (Conn et al., 2011). CATION  
119 EXCHANGER (CAX) are ion transporters located on the tonoplast membrane (Hirschi, 1999; Manohar et al.,  
120 2011) and several studies in *A. thaliana* have suggested they play a critical role in plant adaptation to certain  
121 stresses such as salinity (Cheng et al., 2003; Park et al., 2005). These antiporters also use the driving force of the  
122 proton gradient generated by the vacuolar pumps (V-ATPase and AVP1) to accumulate  $\text{Na}^+$  into the vacuole  
123 against its electrochemical gradient. In addition, the *TWO-PORE CHANNEL 1 (TPC1)* gene encodes for most  
124 prominent cation Slow Vacuolar channel which represents the major cation conductance of the largest organelle  
125 in most plant cells (Kintzer and Stroud, 2016), mainly  $\text{Ca}^{2+}$ , but also other ions such as  $\text{K}^+$  and  $\text{Na}^+$  (Hedrich  
126 and Marten, 2011). In *Arabidopsis*, it has been proven that *TPC1* mediates a voltage-activated  $\text{Ca}^{2+}$  influx in  
127 leaf cells (Furuichi et al., 2001), contributing to the cytosolic calcium elevation and therefore to stress signalling  
128 (Hedrich and Marten, 2011; Choi et al., 2014).

129 CALCINEURIN B-LIKE PROTEIN 10 (CBL10), the last CBL family member to be identified so far, has  
130 also been involved in the regulation of salt stress response in *A. thaliana* (Kim et al., 2007; Quan et al., 2007).  
131 CBLs are EF-hand  $\text{Ca}^{2+}$  protein sensors and upon  $\text{Ca}^{2+}$  binding, they undergo conformational changes to

132 associate with a group of CBL-INTERACTING PROTEIN KINASES (CIPKs) (for review see Kolukisaoglu et  
133 al., 2004; Luan, 2008; Kim, 2013). Different combinations of CBLs and CIPKs complexes may generate  
134 temporal and spatial specificity in  $\text{Ca}^{2+}$  signalling, integrating various stimuli to determine cellular responses  
135 (Batistic et al., 2010). Previous studies have determined that CBL10 interacts and recruits CIPK24 (SOS2)  
136 towards the tonoplast, speculating that the CBL10-CIPK24 complex might phosphorylate and activate a  
137 tonoplast  $\text{Na}^+$  channel or transporter yet unknown in order to transport cytosolic  $\text{Na}^+$  into the vacuole (Kim et  
138 al., 2007; Quan et al., 2007; Waadt et al., 2008; Lin et al., 2009). Moreover, a recent study has also  
139 demonstrated that *A. thaliana* CBL10 is critical for reproductive development under salt stress, although this  
140 function occurs independently from SOS2 interaction (Monihan et al., 2016). Likewise, Kang and Nam (2016)  
141 have provided an additional explanation for the positive role of CBL10 in salt tolerance by regulating sensitivity  
142 to brassinosteroids. Following the initial discovery of CBL10 in *A. thaliana*, a homologue has been reported in  
143 *Populus* and attributed similar functions (Tang et al., 2014). A CBL10 homologue has also been reported in  
144 tomato and its function in pathogen response within the reactive oxygen species signaling pathway has been  
145 demonstrated (de la Torre et al., 2013). However, the role for *SICBL10* in the regulation of abiotic stress  
146 responses in tomato remains unexplored. Furthermore, the relationship of *CBL10* gene with other genes  
147 involved in the regulation of ion homeostasis (*SOS1*, *HKT1s*, *AVP1*, *VHA-A1* and *TPC1*) has neither been  
148 established so far in any species. This study reports the identification of the tomato *Slcbl10* knock-out mutant  
149 which exhibited very high salt-sensitivity. The functional characterization of this mutant revealed a new role of  
150 the *SICBL10* gene in the salt tolerance of tomato by balancing  $\text{Na}^+$  and  $\text{Ca}^{2+}$  homeostasis.

151

## 152 **RESULTS**

### 153 **Isolation of the *pms916* salt hypersensitive T-DNA mutant and molecular cloning of the tagged gene**

154 An *in vitro* phenotypic screening to identify mutants with altered salt stress responses was performed in a  
155 tomato T-DNA mutant collection by growing T2 segregating families in a basal culture medium (SCM)



156 supplemented with 100 mM NaCl (for details, see Materials and Methods). As a result, the *pms916* (*protecting*  
157 *meristem from salt stress 916*) mutant was isolated, which exhibited abnormal thickening of the hypocotyl,  
158 severe inhibition of vegetative development and a collapse of the apical meristem after 20 days of salt treatment  
159 (20 DST; Fig. 1A). A similar mutant phenotype was observed in three additional repeated assays (Experiments  
160 E1, E2 and E3 in Supplemental Table S1) performed using identical salt stress conditions. Subsequently, the  
161 salt-sensitivity of the *pms916* mutant was corroborated *in vivo* by growing T2 plants under greenhouse  
162 conditions (Experiments E4 and E5 in Supplemental Table S1). In all *in vitro* and *in vivo* experiments, genetic  
163 analysis indicated that *pms916* mutation was inherited as monogenic and recessive (Supplemental Table S1).

164 Southern blot analysis showed that the original T1 plant carrying the *pms916* mutation harboured three T-  
165 DNA copies (Fig. 1B). To identify lines with a single T-DNA insertion, T3 progenies were used for kanamycin  
166 sensitivity test. The results showed a 3:1 (tolerant:sensitive) segregation for kanamycin response in four of the  
167 ten progenies evaluated, indicating a single-locus insertion of the T-DNA. These four T3 progenies were grown  
168 *in vitro* under identical salt conditions as described above (SCM + 100 mM NaCl). From each T3 progeny, a  
169 single plant showing a *pms916* mutant phenotype was analysed by Southern blotting. The results indicated that  
170 two T-DNA insertions were present in all mutant plants (Fig. 1B). Genomic regions flanking T-DNA insertions  
171 were cloned by anchor-PCR, and the sequencing analysis revealed that the two T-DNA copies were inserted in  
172 a head-to-tail tandem orientation (Fig. 1C). Hence, both T-DNA copies were inherited as a single locus, which  
173 agreed with the results of the kanamycin sensitivity test. The T-DNA tandem insertion was located on  
174 chromosome 8 of the tomato genome, within the *CALCINEURIN B-LIKE PROTEIN 10* (*SICBL10*) gene  
175 (*Solyc08g065330*). The inserted fragment caused a deletion of 1,836 bp, between 1,634 bp upstream and 202 bp  
176 downstream of the translation start codon of the *SICBL10* gene (Fig. 1C), preventing, in all likelihood, the  
177 translation of a functional protein.

178 A PCR co-segregation analysis was then carried out to determine whether the T-DNA insertion correlated  
179 with the mutant phenotype. For this purpose, the *SICBL10* genotype of 25 T2 individuals was determined using  
180 G-F, G-R, and T2-R primer combinations (Fig. 1, C and D, and Supplemental Table S2). Among the 18 wild-

181 type (WT) individuals, 14 plants were heterozygous and 4 homozygous for the WT allele, while the remaining 7  
182 mutant plants carried the mutant allele in the homozygous state (Fig. 1D). These results strongly supported that  
183 the disruption of the *SICBL10* gene by the T-DNA insertion was responsible for the *pms916* mutant phenotype  
184 and therefore, the tomato *pms916* insertional mutant was renamed as *Slcbl10*.

185

### 186 **Phenotypic characterization of *Slcbl10* mutant plants**

187 In order to more deeply characterize the *Slcbl10* mutant phenotype, T3 homozygous and azygous lines for the  
188 *Slcbl10* mutation, both belonging to the same T2 family, were grown in a hydroponic system as described in the  
189 Materials and Methods section. In the absence of salt stress, *Slcbl10* mutant plants grown normally with the  
190 only exception of a slight chlorosis at the margins of some young leaflets at the moment when plants have  
191 developed a few number of leaves. The sensitive phenotype was accentuated as mutant plants grew, showing  
192 bulging and thickening of the leaflets forming the shoot apex (Supplemental Fig. S1).

193 Short-term hydroponic salt treatment (HST) assays showed that salinity caused severe damages in the aerial  
194 part of *Slcbl10* mutant plants, in both young and adult plants (for further details Materials and Methods section).  
195 Vegetative growth of *Slcbl10* homozygous plants was arrested at young stages (HSTy assay) and they showed  
196 swelling and curved appearance of leaves, chlorosis at edge of leaflet and apical collapse (Fig. 2A). Salt  
197 treatment also induced growing abnormalities in *Slcbl10* adult plants (HSTa assay). Thus, after 2 DST, mainly  
198 young apical tissues became burnt and wilted, and subsequently mutant plants stopped growing as a  
199 consequence of apical collapse just after 6 DST (Fig. 2B). However, it was surprising that leaves and stems at  
200 basal positions on *Slcbl10* mutant plants did not show evident symptoms of salt sensitivity. Instead; their  
201 external appearances were similar to that of WT plants after 6 DST (Fig. 2B), indicating that in a first instance,  
202 loss of *SICBL10* function mainly affects shoot apex and growing tissues although finally the whole plant is  
203 affected and dies from apical collapse.

204 To corroborate that the salt hypersensitivity phenotype of the *Slcbl10* mutant was due to the loss of *SICBL10*  
205 gene function, two clonal replicates of 14 independent RNAi *SICBL10* lines and 13 independent regenerants,

206 these latter obtained under the same conditions except for the use of the RNAi gene construct (control plants),  
207 were grown and characterized under hydroponic salt treatment (HSTa assay conditions). All RNAi *SICBL10*  
208 lines displayed salt stress sensitivity, showing an altered phenotype almost equal to that of mutant plants (Fig.  
209 2C), including decreased fresh weight of shoots and roots (Fig. 2D). These results confirmed that the T-DNA  
210 mutation affecting the *SICBL10* gene was responsible for the salt-hypersensitivity initially observed in the  
211 *pms916* mutant.

212

### 213 **Functional complementation of the *Arabidopsis cbl10* mutant line**

214 In order to test whether the *SICBL10* gene is an orthologue of the *Arabidopsis CBL10*, the entire ORF  
215 corresponding to the putative *SICBL10* was cloned under the control of a 35S promoter. This construct was used  
216 to transform and test a functional complementation of the *Arabidopsis cbl10* knock-out T-DNA line (Quan et  
217 al., 2007). Salt tolerance of three independent transgenic lines overexpressing *SICBL10* in a *cbl10* genetic  
218 background was compared to that of wild-type (Col-0) and the *cbl10* mutant plants (Fig. 3A). Whilst growth in  
219 100 mM NaCl is more severely compromised in the *cbl10* mutant than in WT plants, heterologous expression of  
220 *SICBL10* in this mutant genetic background restores growth to WT levels (Fig. 3B). Previous studies have  
221 shown that despite being hypersensitive to salinity, the *Arabidopsis cbl10* mutant accumulated less Na<sup>+</sup> after  
222 high salt exposure (Kim et al., 2007). Accordingly, results here obtained demonstrated that the expression of  
223 *SICBL10* restored Na<sup>+</sup> accumulation to WT levels in *cbl10* mutant plants (Fig. 3C). In conclusion, *SICBL10* was  
224 able to reiterate *CBL10* function in *Arabidopsis* indicating that *SICBL10* is a true orthologue of the *CBL10* gene.

225

### 226 **The *SICBL10* gene is differentially expressed in tomato tissues, and is induced by salt stress**

227 Changes of *SICBL10* expression induced by salt stress were further analysed in adult WT plants grown in a  
228 hydroponic system (HSTa assay conditions). Salinity induced an increase of *SICBL10* expression in all tissues  
229 analysed (Fig. 4A). In shoot, the highest expression levels were detected in upper adult leaves (3-fold increase),

230 followed by young leaves and stems (2-fold increase). The lowest *SICBL10* expression was found in roots,  
231 although a significant increase was also detected in salt-treated plants.

232 The temporal effect of salt stress on *SICBL10* expression was analysed in the first developed leaf of WT  
233 plants from the same experiment mentioned above (Fig. 4B). Transcript levels of *SICBL10* were significantly  
234 induced by salt treatment after 12 h, reaching the maximum levels between 24 and 48 h. Later, *SICBL10*  
235 expression decreased to the basal levels found in the absence of salt stress after 60 h of treatment. At 6 DST, a  
236 further increase of *SICBL10* expression was observed, therefore suggesting that two phases of induction may  
237 occur during exposure to salt stress.

238

#### 239 **Na<sup>+</sup> distribution pattern is altered in *Slcbl10* mutant plants**

240 To ascertain whether the salt sensitivity phenotype was associated with changes in Na<sup>+</sup> distribution patterns  
241 induced by salt stress, ion contents were analysed in several adult plant tissues from the HSTa assay (Fig. 5A).  
242 Results showed that although Na<sup>+</sup> uptake at whole level was lower in *Slcbl10* mutant than in WT plants (25%  
243 and 20% lower in mutant after 2 DST and 6 DST, respectively), the Na<sup>+</sup> distribution pattern along the mutant  
244 plant was completely altered. In WT plants, Na<sup>+</sup> is preferentially accumulated in roots, and later in adult leaves  
245 and stems to prevent Na<sup>+</sup> from reaching toxic levels in young developing tissues. In fact, the lowest Na<sup>+</sup>  
246 accumulation was found in the shoot apex of WT plants in salt conditions. Contrarily, the *Slcbl10* mutant did  
247 not retain Na<sup>+</sup> properly in roots or in adult leaves or stems as 30% less Na<sup>+</sup> is detected in these tissues, and  
248 therefore similar Na<sup>+</sup> contents were found along the mutant plants. The incapacity of the *Slcbl10* mutant to  
249 retain Na<sup>+</sup> in adult vegetative tissues allows the ion to reach the apex in higher concentration, 70% higher than  
250 in WT, after 6 DST.

251 An opposite tendency was observed for K<sup>+</sup> distribution. Thus, during salt treatment, the K<sup>+</sup> content was  
252 higher in roots, upper adult leaves and stems of mutant plants than in WT plants, while a similar K<sup>+</sup> content was  
253 detected in the apex (Supplemental Fig. S2). This fact, promoted that the Na<sup>+</sup>/K<sup>+</sup> ratio was lower in roots and  
254 upper adult leaves of the *Slcbl10* mutant, but higher in the apex due to a higher Na<sup>+</sup> accumulation in these

255 tissues (Fig. 5B). Together these results strongly evidence that salt stress induces significant alterations in Na<sup>+</sup>  
256 and K<sup>+</sup> homeostasis of *Slcbl10* mutant plants.

257 Transcript levels of main genes involved in Na<sup>+</sup> homeostasis were analysed in the first developed leaf and  
258 roots (Fig. 5C). With this purpose, expression of genes responsible for the uptake and long-distance Na<sup>+</sup>  
259 transport in tomato, *SISOS1* and *SIHKT1s*, (Olias et al., 2009; Asins et al., 2013), as well as genes involved in  
260 Na<sup>+</sup> accumulation into vacuole, *LeNHX3*, *LeNHX4* (Galvez et al., 2012), *SIAVP1* and *SIVHA-A1* genes (Gaxiola  
261 et al., 2007) were determined. In addition, expression of *SISOS2* gene, which has been related to both long-  
262 distance Na<sup>+</sup> transport and Na<sup>+</sup> accumulation process (Huertas et al., 2013; Olias et al., 2009), was also  
263 analysed. Although no differences in the expression levels of these genes were detected between *Slcbl10* mutant  
264 and WT plants when they were grown under control conditions, some significant changes were found when  
265 plants grew under salt stress, mainly affecting leaf tissue (Fig. 5C). Salinity induced up-regulation of all  
266 analysed genes involved in Na<sup>+</sup> compartmentalization, i.e. *LeNHX3*, *LeNHX4*, *SISOS2*, *SIAVP1* and *SIVHA-A1*,  
267 in WT but not in mutant leaves where only *LeNHX3* and *SIVHA-A1* were up-regulated. Furthermore, the  
268 *SIHKT1;2* gene was significantly down-regulated in leaves of mutant plants. In roots, the only remarkable  
269 difference was the induction by salinity of *SISOS1* expression in mutant but not in WT plants, which indicated  
270 that Na<sup>+</sup> extrusion from root to external medium was increased when *SICBL10* expression is knocked-out  
271 (Supplemental Fig. S3).

272

### 273 **Disruption of *SICBL10* gene affects Ca<sup>2+</sup> homeostasis under salt stress**

274 Another singular feature of *Slcbl10* mutant extracted from ion analysis was an altered Ca<sup>2+</sup> distribution pattern  
275 under salinity (Fig. 6A). Thus, while the hydroponic salt treatment (HSTa assay) caused a significant reduction  
276 of Ca<sup>2+</sup> content in both stems and upper adult leaves of WT plants after 6 DST, no significant changes of Ca<sup>2+</sup>  
277 content were observed in *Slcbl10* mutant plants. Consequently, Ca<sup>2+</sup> content was 80% and 60% higher in stem  
278 and upper adult leaves, respectively, in *Slcbl10* than in WT plants.

279 The higher  $\text{Ca}^{2+}$  levels detected in upper adult leaves and stem of *Slcbl10* mutant plants could be due to  $\text{Ca}^{2+}$   
280 retention or to an increased  $\text{Ca}^{2+}$  transport from roots to shoots during salt treatment. In order to check these two  
281 possibilities reciprocal grafting experiments were performed between WT and *Slcbl10* plants, and  $\text{Ca}^{2+}$  contents  
282 were measured in grafted plants grown under hydroponic salt treatment (HSTa assay conditions; Fig. 6B). Level  
283 of  $\text{Ca}^{2+}$  was significantly higher in leaves of grafted plants using *Slcbl10* as scion independently of the rootstock  
284 background, while a similar decrease of  $\text{Ca}^{2+}$  content was found in leaves when WT scion was grafted on either  
285 WT or mutant rootstock. In addition, no significant differences of  $\text{Ca}^{2+}$  content were found in roots of the  
286 different combinations. Therefore, it is possible to conclude that the higher  $\text{Ca}^{2+}$  content found in *Slcbl10*  
287 mutant organs was not due to a higher  $\text{Ca}^{2+}$  transport from root to shoot but, most likely, to retention in leaves  
288 of  $\text{Ca}^{2+}$  stores, which did not diminish under salinity.

289 Under calcium deficit conditions, such as those promoted by salinity (White and Broadley, 2003), plants  
290 need to mobilize their calcium reservoirs to ensure fruit development and yield. Therefore, possible effects on  
291 fruit yield promoted by  $\text{Ca}^{2+}$  reservoirs improperly retained in leaves and stems of *Slcbl10* plants were  
292 analysed in a long term salt treatment assay in a greenhouse (GST assay conditions; see Materials and  
293 Methods). Fruit yield and blossom end rot (BER) incidence, the latter being a well- known symptom of  $\text{Ca}^{2+}$   
294 deficiency disorders in tomato fruit (de Freitas et al., 2014; Zhai et al., 2015), were determined in adult plants  
295 after 50 DST (Fig. 6C). A considerably decrease of fruit production and higher BER incidence (7-fold) was  
296 detected in *Slcbl10* plants with respect to WT). In addition, other phenotypic alterations that coincided with  
297 those promoted by  $\text{Ca}^{2+}$  deficiency were observed in long term salt-treated *Slcbl10* and RNAi *SICBL10* plants,  
298 among others, reduced growth of the apical meristem, small leaves with evident chlorosis symptoms at their leaf  
299 edges and thickened petioles and stems (Supplemental Fig. S4 and Fig. S5). Taken together, these results  
300 indicated that under salinity conditions,  $\text{Ca}^{2+}$  reservoirs are less available in *Slcbl10* plants than in WT, thus  
301 limiting their proper development and productivity.

302 To corroborate that the low  $\text{Ca}^{2+}$  availability is responsible for the growth restriction of *Slcbl10* mutant in salt  
303 stress conditions, an *in vitro* assay was carried out using 1 mM suboptimal  $\text{Ca}^{2+}$  concentration. Under these

304 conditions, the *Slcbl10* mutant showed higher sensitivity to a Ca<sup>2+</sup> deficiency condition (Supplemental Fig. S6,  
305 A and B). The first Ca<sup>2+</sup> deficiency symptom observed was a collapse of the subapical shoot region resulting in  
306 a constriction necrosis below the shoot tip, followed by the apical meristem senescence. Light microscopic  
307 analysis also revealed significant alterations affecting SAM morphology and ground cells of *Slcbl10* mutant  
308 plants (Supplemental Fig. S6, C and D). In addition, swollen cells were observed in the submeristematic region  
309 immediately below the collapsed zone leading to thickened stems (Supplemental Fig. S6E) whose appearance  
310 strongly resembled that observed in *Slcbl10* young plants grown under salt conditions (Fig. 2). These results  
311 strongly support that tomato plants lacking *SICBL10* are not able to balance their development under Ca<sup>2+</sup>  
312 deficient conditions.

313

#### 314 **Expression pattern of key genes involved in vacuolar fluxes of Ca<sup>2+</sup>**

315 To ascertain how *SICBL10* might be involved in the mobilization of Ca<sup>2+</sup> stores, and taken into account that the  
316 vacuole is by far the largest intracellular Ca<sup>2+</sup> store in mature cells (Peiter, 2011), the expression profile of key  
317 genes involved in Ca<sup>2+</sup> fluxes were analysed. Concretely, transcript accumulation of *CAX1*, *AVP1* and *VHA-A1*  
318 genes, all required for Ca<sup>2+</sup> compartmentalization into the vacuole (Pittman, et al., 2009), and *TPCI* involved in  
319 Ca<sup>2+</sup> release from vacuole (Herdrich and Marten, 2011), were measured in upper adult leaves of *Slcbl10* mutant  
320 and WT plants grown under HSTa assay conditions. Given the essential role of Ca<sup>2+</sup> as a second messenger of  
321 signalling stress, gene expression analyses were performed at early and later steps of salt treatment (Fig. 7). In  
322 WT plants, salinity induced a down-regulation of *SICAX1*, while *SITPCI*, the main responsible channel for the  
323 release of Ca<sup>2+</sup> from vacuole, was up-regulated. The lowest levels of *SICAX1* transcripts were detected after 48h  
324 of salt treatment which remained low until the end of treatment. *SITPCI* registered two maximum levels of  
325 expression, one soon after 48 hours and the other later, at the end of salt treatment. In *Slcbl10* mutant plants,  
326 expression of *SITPCI* was not induced by salinity, but it was down-regulated (65% reduction) after 48 hours of  
327 salt exposure. Moreover, *SICAX1* expression was more pronounced and earlier repressed in *Slcbl10* mutant than  
328 in WT plants. Indeed, after 60 hours of salt exposure, the level of *SICAX1* transcripts was almost null in the

329 mutant (98% of inhibition). The expression pattern of these genes in WT indicated that salinity induced an  
330 efflux of  $\text{Ca}^{2+}$  from vacuole, while in mutants this efflux may be impaired by the strong down-regulation of  
331 *TPCI*.

332 As regards the vacuolar proton-pumps coded by *SIAPVI* and *SIVHA-AI* genes, salinity induced a similar  
333 profile expression to that described for *SITPCI* in wild-type plants, as a peak of induction was detected at 48  
334 hours of salt treatment (Fig. 7). However, the level of transcripts of both *SIAPVI* and *SIVHA-AI* genes were  
335 significantly lower in *Slcbl10* mutant plants than in WT. It is interesting to highlight that the expression patterns  
336 of *SITPCI* and the two vacuolar proton pumps, *SIAPVI* and *SIVHA-AI* followed a very similar temporal pattern  
337 expression, suggesting that they may cooperate to regulate proper  $\text{Ca}^{2+}$  flux in the vacuole under salt stress in  
338 tomato.

339

#### 340 ***SICBL10* gene is needed to maintain a proper ratio $\text{Na}^+/\text{Ca}^{2+}$ in flowers and apex under salinity**

341 It is known that under salinity conditions, the maintenance of a proper  $\text{Na}^+/\text{Ca}^{2+}$  low ratio in growing tissues,  
342 such as shoot apex and flowers, is essential to maintain plant growth (Manaa et al., 2013). Thus, in order to  
343 ascertain when the lack of *SICBL10* gene prevents the maintenance of a proper  $\text{Na}^+/\text{Ca}^{2+}$  ratio that ensures the  
344 growth in tissues such as apex and flowers under salinity,  $\text{Na}^+/\text{Ca}^{2+}$  ratio was assessed in WT, *Slcbl10* mutant  
345 and RNAi *SICBL10* plants. After 6 DST  $\text{Na}^+$  and  $\text{Ca}^{2+}$  contents were analysed in upper adult leaf, apex and  
346 flowers (first flower truss immediately below 1<sup>st</sup> fully developed leaf). In RNAi *SICBL10* and *Slcbl10* mutant  
347 plants, a higher  $\text{Ca}^{2+}$  content but a lower  $\text{Na}^+$  content were registered in upper adult leaves as compared to WT  
348 (Fig. 8, A and B). Contrarily, in apex and flowers,  $\text{Na}^+$  levels increased and  $\text{Ca}^{2+}$  levels decreased both in  
349 *Slcbl10* mutant and in RNAi plants (Fig. 8, A and B), causing the  $\text{Na}^+/\text{Ca}^{2+}$  ratios in these tissues to be  
350 improperly high (Fig. 8C), which might be the ultimate responsible factor for the observed alterations in  
351 mutants cultivated under salinity.

352



353 **DISCUSSION**

354 This study reports the identification and functional characterization of the tomato *Slcbl10* knock-out mutant  
355 identified from a screening of a T-DNA tomato mutant population (Pineda et al., 2012; Pérez-Martín et al.,  
356 2017). Through an anchor-PCR approach, *SICBL10* was identified as the tagged gene responsible for the salt  
357 hypersensitive mutant phenotype. Molecular complementation experiments proved that *SICBL10* is orthologous  
358 to the *A. thaliana* *CBL10* gene, and encodes a calcium sensor CALCINEURIN B-LIKE PROTEIN 10.  
359 Although *SICBL10* was previously involved in a signaling pathway mediating tomato plant immunity (de la  
360 Torre et al., 2013), its role in regulating abiotic stress has not been studied so far in this model species.

361

362 ***SICBL10* protects growing tissues from salt stress by Na<sup>+</sup> retention in adult tissues**

363 Results here reported indicate that the salt sensitivity phenotype of *Slcbl10* mutant plants (i.e. growth inhibition,  
364 hypocotyl thickening and apical necrosis) was similar both under *in vitro* and *in vivo* stress conditions and that  
365 such phenotype was also corroborated in RNAi *SICBL10* lines. In all cases, the lack of the *SICBL10* finally  
366 drove plants to die from apical collapse (Fig. 2). In addition, expression analysis showed that *SICBL10* was up-  
367 regulated in WT plants cultivated under salinity conditions, the highest expression level being detected in upper  
368 adult leaves close to the shoot apex. Together, these results indicate that transcriptional activity of *SICBL10*  
369 plays a key role in the adaptive response of tomato plants to salt stress by protecting shoot apical meristem and  
370 growing tissues from physiological damages caused by salinity.

371 Previous studies have shown that CBL10 is also involved in salt response in *A. thaliana* (Kim et al., 2007;  
372 Quan et al., 2007) and *Populus* (Tang et al., 2014). Indeed, *Arabidopsis cbl10* mutant plants accumulated lower  
373 Na<sup>+</sup> and a higher K<sup>+</sup> content as a consequence of salt treatment, being the first salt-hypersensitive mutant with a  
374 lower Na<sup>+</sup>/K<sup>+</sup> ratio reported so far (Kim et al., 2007). Here it has been showed that tomato *Slcbl10* mutant also  
375 accumulates lower Na<sup>+</sup> and higher K<sup>+</sup> than wild-type plants; in addition, functional complementation of the  
376 *Arabidopsis cbl10* mutant by *SICBL10* leads to the recovery of Na<sup>+</sup> levels. Under these premises, it is necessary

377 to explain how plants accumulating less Na<sup>+</sup>, as are the cases for *Slcbl10* and *cbl10* mutants, showed a salt-  
378 hypersensitive phenotype when the opposite would be expected. A precise dissection of Na<sup>+</sup> relative content in  
379 young *versus* adult leaves as well as in leaves *versus* stems in tomato allowed for the elucidation of the role  
380 played by *SICBL10* in Na<sup>+</sup> homeostasis. It is known that the mechanism of salinity tolerance in tomato involves  
381 a preferential Na<sup>+</sup> accumulation in adult leaves and stems, which prevents Na<sup>+</sup> from reaching the shoot apex  
382 (Cuartero et al., 2010). Our results proved that this physiological mechanism was totally altered in *Slcbl10*  
383 mutant, which was not able to retain Na<sup>+</sup> in adult tissues. This alteration leads to a 7-fold increase in Na<sup>+</sup>  
384 content that reaches the shoot apex, which results in an inadequate high Na<sup>+</sup>/K<sup>+</sup> ratio in growing tissues.  
385 Changes in Na<sup>+</sup>/K<sup>+</sup> ratios are consistent with the physiological damages detected in the apical part of mutant  
386 plants and strongly support a functional role of the *SICBL10* gene in protecting shoot apex and developing  
387 tissues from salt stress conditions.

388

### 389 ***SICBL10* function is required for Na<sup>+</sup> compartmentalization into vacuole**

390 In the cytoplasm, inappropriate Na<sup>+</sup> levels cause important metabolic alterations as this ion inhibits enzyme  
391 activity (Maathuis, 2009); for that reason, cytoplasmic Na<sup>+</sup> content have to be kept at low level by exporting  
392 Na<sup>+</sup> into the vacuole (Albaladejo et al., 2017). Results from expression analysis revealed that the decreased  
393 capacity of *Slcbl10* plants to retain Na<sup>+</sup> in adult leaf was associated with a significant lower salt-induced  
394 expression of genes involved in Na<sup>+</sup> compartmentalization into vacuole, such as *LeNHX4*, *SlAVP1*, *SIVHA-A1*,  
395 and *SISOS2*. Moreover, in the leaves of *Slcbl10* plants it was observed both a reduced expression of *SIHKT1;2*,  
396 the main responsible for uploading Na<sup>+</sup> from the xylem into the cells (Asins et al., 2013; 2015), as well as an  
397 increase of *SISOS1* gene expression, responsible for Na<sup>+</sup> extrusion from leaf cells to xylem (Olias et al., 2009).  
398 Hence, expression analysis support the hypothesis that Na<sup>+</sup> compartmentalization into vacuoles as well as Na<sup>+</sup>  
399 upload from xylem into cells were severely inhibited in *Slcbl10* mutant plants, while Na<sup>+</sup> extrusion from leaf  
400 cells to xylem was favoured (Fig. 9). Such physiological changes allow the toxic ion to reach the apex and  
401 flowers promoting their collapse and the subsequent death of the plants. Therefore, results indicate that

402 *SICBL10* is needed for regulating Na<sup>+</sup> homeostasis through the activity of genes involved in the  
403 compartmentalization of Na<sup>+</sup> into vacuole.

404 In *Arabidopsis*, the CBL10-SOS2 complex has been proposed as a positive regulator of a still unknown  
405 vacuolar protein triggering Na<sup>+</sup> compartmentalization into vacuoles (Kim et al., 2007; Waadt et al., 2008).  
406 Additionally, it has been determined that SOS2 regulates AtNHX1 antiporter activity (Qiu et al., 2004) and  
407 directly activates the vacuolar H<sup>+</sup> pump V-ATPase (Batelli et al., 2007). However, a previous study in *Populus*  
408 suggested that CBL10 is not directly related to the function of NHX proteins (Tang et al., 2014), which points at  
409 the vacuolar H<sup>+</sup>-pumps as the potential candidates for protein targets of CBL10 (Fig. 9). In tomato, the lack of  
410 *SICBL10* function was associated with a repression of *SISOS2*, and the constitutive expression of *SICBL10*  
411 rescued the phenotype of the *Arabidopsis cbl10* mutant, indicating that the molecular mechanism underlying  
412 Na<sup>+</sup> compartmentalization into vacuole mediated by *SICBL10* may be shared between *Arabidopsis* and tomato.

413

#### 414 ***SICBL10* promotes Ca<sup>2+</sup> mobilization and availability under salt stress conditions**

415 Ca<sup>2+</sup> deficit usually occurs in plants growing in salinized soils, since elevated Na<sup>+</sup> concentrations hinder Ca<sup>2+</sup>  
416 uptake by roots (Zhai et al., 2015), which usually induces a reduction of Ca<sup>2+</sup> content in upper leaves and stem.  
417 Decreased Ca<sup>2+</sup> levels were detected in WT but not in *Slcbl10* mutant plants when they grew under salinity  
418 conditions (Fig. 6). Using reciprocal grafting between WT and the *Slcbl10* mutant, it was also proved that the  
419 higher Ca<sup>2+</sup> levels detected in *Slcbl10* mutant leaves resulted from Ca<sup>2+</sup> retention in these tissues rather than  
420 from a higher Ca<sup>2+</sup> transport from the root to the shoot during salt treatment. Likewise, given that Ca<sup>2+</sup> stores in  
421 apical leaves and stem could be exchanged and mobilized to other tissues (apical meristem, flower and fruit)  
422 according to the physiological Ca<sup>2+</sup> needs of plants (White and Broadley, 2003; Dayod et al., 2010), the  
423 retention of Ca<sup>2+</sup> in *Slcbl10* upper leaves could cause an inefficient supply of Ca<sup>2+</sup> to other demanding tissues,  
424 such as flowers and shoot apex, thus contributing to their collapse under salinity. Several specific abnormalities  
425 have been reported due to Ca<sup>2+</sup> deficit, mainly reduced growth of apical meristems, chlorotic leaves, tissue

426 softening and high BER incidence in fruits (Robertson, 2013; Uozumi et al., 2012; de Freitas et al. 2014).  
427 Therefore, abnormal  $\text{Ca}^{2+}$  retention detected in upper adult leaves may also be responsible for the almost null  
428 production of fruits and high BER incidence detected in *Slcbl10* plants characterized under salinity conditions.

429 The fact that the *Slcbl10* mutant was not able to balance its development in a  $\text{Ca}^{2+}$  deficient medium (1 mM  
430  $\text{Ca}^{2+}$ ) also indicates that *SICBL10* is required for an appropriate  $\text{Ca}^{2+}$  partitioning in tomato plants. Results  
431 showed that under suboptimal  $\text{Ca}^{2+}$  concentration, *SICBL10* promotes the adequate expansion and division of  
432 pith cells below the shoot apical meristem. Indeed, the truncation of *SICBL10* resulted in the collapse of  
433 subapical cells, and finally caused the death of the shoot apical meristem; said symptoms have been previously  
434 described as resulting from a suboptimal concentration of calcium reaching growing tissues (Busse, 2008).  
435 Therefore, under salt stress conditions, *SICBL10* gene function makes it possible that  $\text{Ca}^{2+}$  reservoirs can be  
436 mobilized, a feature which is essential to regulate plant growth and survival of developing tissues.

437

#### 438 ***SICBL10* and *SITPCI* cooperate in the proper $\text{Ca}^{2+}$ release**

439 The vacuole is by far the largest intracellular  $\text{Ca}^{2+}$  store in mature cells (Peiter, 2011), and constitutes the main  
440  $\text{Ca}^{2+}$  reservoirs from which  $\text{Ca}^{2+}$  is exchanged and mobilized according to the physiological  $\text{Ca}^{2+}$  needs of plant  
441 (White and Broadley, 2003; Dayod et al., 2010). Expression profile of key vacuolar genes involved in  $\text{Ca}^{2+}$   
442 homeostasis suggest that the mechanism required to originate  $\text{Ca}^{2+}$  fluxes in vacuole was severely affected when  
443 *Slcbl10* plants grew in salt stress conditions (Fig. 9). Thus, salinity did not induce the expression of *SIAPV1* and  
444 *SIVHA-A1* genes, which implies that the proton gradient, which is necessary to energize the  $\text{Ca}^{2+}$  transport  
445 towards the vacuole through CAX1 antiporters (Manohar et al., 2011), was impaired by the lack of *SICBL10*  
446 gene function. Also, the stronger inhibition of *SICAX1* observed in *Slcbl10* mutant plants could contribute to  
447 altering the proton gradient. Indeed, an indirect feedback mechanism has been proposed between CAX  
448 transporters (CAX1, CAX2, CAX3) and  $\text{H}^+$ -pump V-ATPase in *Arabidopsis*, which would generate  $\text{H}^+$  flux  
449 across the tonoplast (Cheng et al., 2003). Since TPC1 has been reported as the main responsible factor for

450 promoting  $\text{Ca}^{2+}$  efflux from vacuole to cytoplasm in leaf cells (Furuichi et al., 2001), the lower  $\text{H}^+$  pump into  
451 the vacuole of *Slcbl10* plants might result in an inefficient opening of the SITPC1 channel since a low luminal  
452 pH is required to regulate the aperture of this channel (Kintzer and Stroud, 2016). Moreover, the fact that the  
453 expression of *SITPC1* was not induced by salinity in *Slcbl10* mutant, as occurred in WT plants, together with a  
454 probable loss of efficiency for opening of SITPC1 channel suggest that in mutant plants, the  $\text{Ca}^{2+}$  release from  
455 vacuole induced by salinity is disturbed, which in turn could cause a defective calcium mediated salt-stress  
456 signalling and therefore, salt sensitivity (Choi et al., 2014). Indeed, it has been proven that TPC1 is involved in  
457 the generation of  $\text{Ca}^{2+}$  cytoplasmic concentration elevation waves directed to stress signalling purposes (Evans  
458 et al., 2016). Based on this study's results, it seems possible to suggest that SICBL10 plays a role in  $\text{Ca}^{2+}$ -  
459 mediated stress signalling through direct or indirect TPC1 channel regulation (Fig. 9). Direct regulation of  
460 TPC1 by CBL10 would imply that TPC1 is a target for the CBL10-CIPK24 complex to be phosphorylated and  
461 activated. In support of that hypothesis, it has been proposed that the TPC1 channel is regulated by  
462 phosphorylation (Kintzer and Stroud, 2016). Indirect regulation of TPC1 by CBL10 could be mediated by the  
463 acidification of vacuole through the regulation of vacuolar  $\text{H}^+$ -pumps, as a low pH is required to open the  
464 channel (Kintzer and Stroud, 2016). In such a way, SlAVP1 or SlV-ATPase would be the potential target for  
465 SICBL10, which would agree with the mechanism discussed for  $\text{Na}^+$  compartmentalization (Fig. 9).

466 The role of *SICBL10* in  $\text{Ca}^{2+}$  releases from vacuole could also contribute to adaptation mechanism to salinity,  
467 allowing mobilization of  $\text{Ca}^{2+}$  vacuolar stores in leaf cells towards fast-growing tissues in order to compensate  
468 for the lower  $\text{Ca}^{2+}$  uptake by root under salinity. The hypothesis of a double function of SICBL10, although  
469 associated with the same mechanism (regulation of  $\text{Ca}^{2+}$  fluxes in vacuole), is supported by the profile  
470 expression registered in WT tomato leaves during salt treatment, in which two induction phases of expression  
471 were detected. The first induction took place during short-time periods (after 24 h of salt treatment) which could  
472 be involved in the signaling of the salt stress process. Later, a second increase of expression could be attributed  
473 to an increasing  $\text{Ca}^{2+}$  demand by fast-growing tissues as a consequence of  $\text{Ca}^{2+}$  deficiency caused by salinity

474 (Fig. 9). The same expression profile was recorded by *SITPC1*, *SIAVP1* and *SIVHA-A1* which reinforces the idea  
475 of a functional relationship between these genes.

476

## 477 CONCLUSIONS

478 This study has proved that the *SICBL10* gene function is required to maintain a proper  $\text{Na}^+/\text{Ca}^{2+}$  ratio in growing  
479 tissues allowing plant growth under salt stress conditions. Although the functional role of CBL10 in controlling  
480  $\text{Na}^+$  homeostasis has been previously demonstrated in *Arabidopsis* (Kim et al., 2007), the regulation of  $\text{Ca}^{2+}$   
481 homeostasis by CBL10 has not been proposed until now. Nevertheless, Monihan et al., (2016) determined that  
482 CBL10 is critical for reproductive development under salt stress conditions and detected a higher  $\text{Na}^+$  and lower  
483  $\text{Ca}^{2+}$  accumulation in *Arabidopsis* flowers. Such results together with the functional complementation of the  
484 *Arabidopsis cbl10* mutant phenotype by *SICBL10* strongly support that *SICBL10* is a true orthologue of the  
485 *Arabidopsis CBL10* and its function is conserved. Thus, it is proposed that the mechanism by which SICBL10  
486 participates in salt tolerance mechanism is directly related to the regulation of  $\text{Na}^+$  and  $\text{Ca}^{2+}$  fluxes in the  
487 vacuole of leaf cells, through the activation of a tonoplast target, being the cation channel SITPC1 and the two  
488 vacuolar  $\text{H}^+$ -pumps, SIAVP1 and SIV-ATPase the potential targets of SICBL10 (Fig. 9). Accordingly, under  
489 salinity conditions, CBL10 confers to adult leaves the capacity to retain  $\text{Na}^+$  avoiding toxic ion accumulation in  
490 young developing tissues as well as facilitates activation of  $\text{Ca}^{2+}$  release from vacuoles in leaves  
491 counterbalancing  $\text{Ca}^{2+}$  deficiency caused by salt stress.

492

## 493 MATERIALS AND METHODS

### 494 Screening and identification of *pms916* (*Slcbl10*) tomato mutant

495 The tomato (*Solanum lycopersicum* L.) cv Moneymaker was used to generate a collection of T-DNA mutants by  
496 means of the enhancer trap vector pD991 (Atarés et al., 2011; Pineda et al., 2012; Campos et al., 2016; Pérez-  
497 Martín et al., 2017). The *in vitro* screening of 1200 T2 families of tomato T-DNA lines (10-12 plants per

498 family) grown in basal culture medium (SCM) supplemented with 100 mM NaCl led to the detection of a  
499 mutant initially named *pms916* (*protecting meristem from salt stress 916*) due to its hypersensitive phenotype to  
500 salt stress. To estimate the number of inserts bearing a functional *NPTII* marker gene, a segregation analysis of  
501 T2 progeny in kanamycin-containing medium (KCM) consisting of Murashige and Skoog (MS) salts  
502 (Murashige and Skoog, 1962), sucrose ( $10 \text{ g l}^{-1}$ ) and kanamycin  $100 \text{ (mg l}^{-1}\text{)}$  was carried out. The identification  
503 of the insert responsible for the mutation and the co-segregation analysis between the insert and the mutant  
504 phenotype were performed by segregation analysis with T2 and T3 progenies in both kanamycin-containing  
505 medium (KCM) and NaCl-containing medium (SCM). To corroborate the *in vitro* salt sensitivity phenotype of  
506 the *pms916* mutant, two new experiments were conducted under *in vivo* conditions. In both experiments, pre-  
507 germinated seeds of the T2 segregating progeny were sown into pots containing coconut fiber and grown under  
508 controlled climatic conditions:  $26 \pm 3 \text{ }^\circ\text{C}$  day/ $18 \pm 1 \text{ }^\circ\text{C}$  night and extra lighting provided by wide-spectrum  
509 tubes ( $450 \mu\text{mol s}^{-1} \text{ m}^{-2}$ ; Gro-lux, Sylvania, Germany) to expose plants to 16 h day length. To assess salt  
510 hypersensitivity, T2 plants were irrigated with half-strength Hoagland solution (Hoagland and Arnon, 1950).  
511 Salt treatment (100 mM NaCl) was initiated when the plants had developed two true leaves.

512 The number of T-DNA copies was determined by Southern blot hybridization experiments. Genomic DNA  
513 was isolated from young leaves as described by Dellaporta et al. (1983). Ten  $\mu\text{g}$  of genomic DNA were digested  
514 with *EcoRI* and *HindIII* endonucleases, electrophoresed in 0.8% agarose gel and blotted onto Hybond N+  
515 membranes (GE Healthcare - Piscataway, NJ) as described by Ausubel et al. (1993). Hybridization was  
516 performed with a chimeric probe, fusing the complete coding sequence of the *NEOMYCIN*  
517 *PHOSPHOTRANSFERASE II (NPTII)* gene to 811 pb of coding sequence from the endogenous tomato  
518 *FALSIFLORA (FA)* gene, which was employed as hybridization positive control (Yuste-Lisbona et al., 2016).

519

## 520 **Cloning of T-DNA flanking sequences and PCR genotyping**

521 The sequences flanking T-DNA were isolated by anchor-PCR according to the procedure previously established  
522 by Pérez-Martín et al. (2017). The sequences of primers used are listed in Supplemental Table S2. The cloned  
523 sequences were compared with SGN Database (<http://solgenomics.net/>) to assign the T-DNA insertion site on  
524 tomato genome.

525 Co-segregation analysis of the T-DNA insertion site with the mutant phenotype in the T2 progeny was  
526 checked by PCR using i) the specific genomic forward (G-F) and reverse (G-R) primers to amplify the WT  
527 allele (without T-DNA insertion) and ii) one specific genomic primer (G-F) and the specific T-DNA border  
528 primer (T2-R) to amplify the mutant allele (carrying the T-DNA insertion). Primers were designed based on  
529 sequence information available from SGN Database (<http://solgenomics.net/>). The sequences of genotyping  
530 primers used are listed in Supplemental Table S2. Amplification of the genotyping primers was performed in a  
531 30 µl volume using 25 ng of total DNA, 50 ng of each primer, 0.25 mM dNTPs, 2.5 mM MgCl<sub>2</sub>, and 1 U of  
532 REDTaq DNA polymerase (SIGMA-Aldrich) in 1X Taq buffer. DNA was amplified under the following  
533 thermal cycling conditions: 94°C for 5 min, followed by 35 cycles at 94°C for 30 s, 60°C for 30 s, and 72°C for  
534 2 min, and a final extension of 5 min at 72°C. PCR products were analysed in 1% agarose gels in SB buffer (10  
535 mM sodium boric acid) and visualized with ethidium bromide.

536

### 537 **Generation of transgenic tomato lines**

538 In order to generate *SICBL10* silencing lines, a RNA interference (RNAi) approach was followed. With this  
539 aim, a 123-bp fragment of the *SICBL10* cDNA was amplified using the SICBL10-RNAiF and SICBL10-RNAiR  
540 primers (Supplemental Table S2), and the PCR product was cloned in sense and antisense orientation separated  
541 by intronic sequences into the pKANNIBAL vector (Wesley et al., 2001) to generate a pKANNIBAL-SICBL10  
542 plasmid. The resulting plasmid was digested with *NotI*, and the entire construct was cloned into the binary  
543 vector pART27 (Gleave, 1992). In all cases, the binary plasmids generated were electroporated into  
544 *Agrobacterium tumefaciens* LBA 4404 strain for further use in genetic transformation experiments.



545 Agrobacterium-mediated transformation was performed following the protocol described by Gisbert et al.  
546 (2000). Fourteen independent diploid transgenic lines silencing *SICBL10* were generated in tomato. The  
547 *SICBL10* expression level was measured by RT-qPCR as described below. Regenerant plants (control plants)  
548 were also obtained under the same conditions except for the use of the RNAi gene construct.

549

#### 550 ***Arabidopsis thaliana* transformation and complementation test**

551 The *Arabidopsis cbl10* mutant line (SALK\_056042) was kindly donated by Professor Karen Schumaker  
552 (University of Arizona). To generate transgenic lines over-expressing *SICBL10*, a 774 bp fragment was cloned  
553 spanning the entire ORF of *SICBL10* (*Solyc08g065330*) in the vector pK7WG2D.1. The resulting construct was  
554 electroporated into *A. tumefaciens* GV3101 and transformed into *cbl10* mutant by floral dip method (Clough  
555 and Bent, 1998).

556 Seeds were surface-sterilized in 100% hypochlorite sodium for 5 minutes, washed five times in sterilized  
557 water and sown in petri dishes containing 0.5X MS medium supplemented with 1% sucrose and 0.9% agar.  
558 Seeds were stratified for 2 days at 4 °C before growth at 22 °C under long-day photoperiod (16h/8h light/dark).  
559 Five-day-old seedlings were transferred to MS medium supplemented with 100 mM NaCl. Na<sup>+</sup> contents were  
560 determined by atomic emission spectrophotometry.

561

#### 562 **Treatment assays**

563 Tomato WT (cv. Moneymaker), T3 homozygous and azygous plants for the *Slcbl10* mutation, RNAi *SICBL10*  
564 and regenerant plants were used for the phenotypic and physiological characterization of the *Slcbl10* mutant and  
565 the functional analysis of the *SICBL10* gene. Seeds were surface-sterilized briefly with 20% (v/v) commercial  
566 bleach for 15 min, and then washed with sterilized water four times and suspended in sterile water at 4°C for 72  
567 h. Germination was performed in darkness, in a 8:3 (v/v) mixture of peat:perlite, at 28°C temperature and 90%  
568 relative humidity. Seedlings were then maintained in a controlled-environment chamber (8 h/16 h day/night

569 cycle at 345  $\mu\text{mol m}^{-2} \text{s}^{-1}$  light, 23-25 °C, 50 -60% relative humidity) until they reached the desired  
570 developmental stage for each experimental assay. During this period, plants were irrigated daily with half-  
571 strength Hoagland solution (Hoagland and Arnon, 1950).

#### 572 *Hydroponic salt treatment assay (HST) and grafting experiments*

573 Short-term HST assays were performed in a controlled-environment chamber (conditions above described).  
574 Tomato plants were grown hydroponically in an aerated half-strength Hoagland solution. Two types of salt  
575 treatments were performed depending on the development stage of plants: i) young plants at cotyledon stage  
576 were treated at 50 mM NaCl for 24 hours and then at 100 mM for 10 additional days (HSTy assay conditions),  
577 and ii) adult plants at the 5<sup>th</sup> fully developed leaf stage were treated at 100 mM NaCl for 24 hours and then at  
578 200 mM for 5 additional days (HSTa assay conditions). In HSTa assays, shoot and root fresh weights were  
579 taken prior to salt treatment and after 2 and 6 days of salt treatment (DST). Ions content was analysed in root,  
580 stem (taken at the 1<sup>st</sup>-2<sup>nd</sup> leaves insertion), upper adult leaf (1<sup>st</sup> fully developed leaf) and shoot apex (leaf  
581 primordial and apical meristem) at 0 DST and after 6 DST. Expression induction by salinity of interesting genes  
582 was determined in shoot apex, young leaf (not fully developed leaf), upper adult leaf, stem and root of plants  
583 after 2 DST. Additionally, gene expressions were also determined in upper adult leaf after 12, 24, 30, 60 and  
584 144 hours of salt stress. All samples were previously frozen in LN<sub>2</sub> and kept at -80°C until further gene  
585 expression analysis. For each genotype, three biological replicates constituted by five plants each were  
586 analysed. Two independent assays were carried out in the same experimental hydroponic conditions described  
587 above.

588 An additional HSTa assay was performed using reciprocal grafting between WT and *Slcbl10* mutant plants  
589 as well as autografting with WT and *Slcbl10* mutant plants in which Ca<sup>2+</sup> content was analysed in root and  
590 upper adult leaf of grafted plants at 0 DST and after 6 DST.

#### 591 *Greenhouse salt treatment assay (GST)*

592 A long-term salt experiment was conducted in a greenhouse of South-eastern Spain with adult plants. At the 7<sup>th</sup>-  
593 8<sup>th</sup> fully developed leaf stage, WT and *Slcb110* plants were transferred from the controlled culture chamber to a  
594 polyethylene greenhouse and grown on cocoa peat, using a drip irrigation system, as previously described  
595 (García-Abellán et al., 2014). The fertirrigation solution was prepared in 2000-liter tanks with local irrigation  
596 water (Electrical Conductivity (EC) = 0.9 dS m<sup>-1</sup>). Before salt treatment, plants were grown under those  
597 conditions for 21 additional days until 10 leaves were fully developed. Then, fifteen plants per genotype were  
598 salt-treated (100 mM NaCl), keeping fifteen additional plants per genotype growing in the absence of salt. Salt  
599 treatment was performed by adding 100 mM NaCl to the tanks under 30/15 °C day/night temperatures, 40%  
600 relative humidity and 500 μmol m<sup>-2</sup> s<sup>-1</sup> of natural light irradiance. After 50 days, fruits of each plant were  
601 counted (number of fruits), weighed (reproductive biomass) and the BER incidence calculated (percentage of  
602 fruit with BER symptoms).

#### 603 *Calcium deficiency in vitro assay*

604 Pregerminated WT and *Slcb110* mutant seeds were grown on MS medium supplemented with a suboptimal  
605 calcium concentration of 1 mM using calcium chloride as a source. Culture media contained 3 g L<sup>-1</sup> sucrose, 0.1  
606 g L<sup>-1</sup> myo-inositol, and 0.9% agar. The pH was adjusted to 5.6 ± 0.02. Media was autoclaved at 121°C for 20  
607 min before use. Plants were cultured in 20 x 150 mm glass capped tubes containing 10 mL of media. Culture  
608 tubes were placed under 8 h/16 h day/night cycle light at 76 μmol m<sup>-2</sup> s<sup>-1</sup> photosynthetic photon flux density  
609 from cool white fluorescent lamps measured at the top of the culture tubes. The temperature was maintained at  
610 23 ± 2 °C. Fifty plants per genotype were examined after 20 and 35 days of *in vitro* culture. After 20 days of  
611 culture in a suboptimal calcium concentration medium, five shoot tips were taken from each genotype and fixed  
612 with 2.5% glutaraldehyde and 4% paraformaldehyde in 0.1 M sodium phosphate buffer (pH 7.2) for 3 h at 4° C.  
613 Afterwards, samples were washed thrice with phosphate buffer, and then incubated with 1% osmium tetroxide  
614 in the same buffer for 2 h. Subsequently, three washes with phosphate buffer were performed. Fixed tissues  
615 were dehydrated in a graded series of ethanol (35, 50, 70, 96 and 100%), and then infiltrated with a propylene  
616 oxide and JB4 resin mixture. After that, they were immersed in JB4 resin overnight at 4° C and finally

617 transferred to flat embedding molds filled with JB4 resin that polymerized at 68° C for 24 h. Polymerized blocks  
618 were sectioned (0.5–0.7 mm thick) with a Leica EM UC6 ultramicrotome (Leica Mikrosysteme, Vienna,  
619 Austria). The sections were stained for 5 min at 60° C in 1% (w/v) toluidine blue and rinsed with de-ionized  
620 water. Finally, stained sections were observed under light microscopy and digital images were obtained.

621

#### 622 **Ion content analysis**

623 Concentration of Na<sup>+</sup>, K<sup>+</sup> and Ca<sup>2+</sup> was measured in plant material dried for 48 h at 80°C, milled to powder and  
624 digested in a concentrated HNO<sub>3</sub>:HClO<sub>4</sub> (2:1 v/v) solution. Na<sup>+</sup>, K<sup>+</sup> and Ca<sup>2+</sup> were analysed by inductively  
625 coupled plasma spectrometry (ICP) (Ionic Service of CEBAS-CSIC, Murcia, Spain).

626

#### 627 **Gene expression analysis**

628 Different vegetable tissues previously frozen in LN<sub>2</sub> and stored at -80°C were analysed by RT-qPCR. Total  
629 RNA was isolated using a RNeasy kit (Qiagen); contaminating DNA was removed with RNase-free DNase  
630 (DNA-free kit, Ambion) and RNA quality was assessed by electrophoresis on a denaturing agarose gel. Total  
631 RNA was quantified in a GeneQuant II spectrophotometer (Pharmacia Biotech) and 5 µg were used for cDNA  
632 synthesis with the First Strand cDNA Synthesis Kit (Thermo Fisher Scientific). RT-qPCR was performed using  
633 1 µl of undiluted cDNA mixed with iQSyBr Green Supermix (BioRad), and 0.45 µM of forward and reverse  
634 primers using assay conditions as previously described (Asins et al., 2013). All reactions were performed in  
635 triplicate. The presence of a single band on an agarose gel electrophoresis and of a single peak in the melting  
636 temperature curve confirmed the specificity of RT-qPCR amplification. Relative expression data were  
637 calculated as described by Asins et al. (2013) using the tomato elongation factor 1α (*LeEF1α*, acc. AB061263)  
638 as housekeeping gene. The expression level was calculated from  $2^{-\Delta\Delta C_t}$  (Livak and Schmittgen, 2001), using the  
639 expression level of each gene from non-treated untransformed tissue as the calibrator sample. Data were  
640 statistically analysed using the SPSS 13.0 software package. All data are given as mean ± SE of three biological

641 replicates of five plants each. Significant differences among means were analysed by Student's *t* and ANOVA  
642 tests ( $P < 0.05$ ).

643 Specifically, it was evaluated the expression level of *SICBL10* (*Solyc08g065330*), *SISOS1* (*Solyc01g005020*),  
644 *SISOS2* (*Solyc12g009570*), *SIHKT1;1* (*Solyc07g014690*), *SIHKT1;2* (*Solyc07g014680*), *LeNHX3*  
645 (*Solyc01g067710*), *LeNHX4* (*Solyc01g098190*), *SIAPV1* (*Solyc06g068240*), *SIVHA-A1* (*Solyc12g055800*) and  
646 *SITPC1* (*Solyc07g053970*) genes. Regarding tomato CAX homologues, two genes homologous to *Arabidopsis*  
647 *CAX1* and *CAX3*, i.e. *Solyc09g005260* (83.9% and 79.1% similarity to *CAX3* and *CAX1*, respectively) and  
648 *Solyc06g006110* (79.7% and 77.1% similarity to *CAX3* and *CAX1*, respectively) were identified. Out of the two  
649 CAX genes analysed, only *Solyc06g006110* was responsive to salinity, and therefore it was named as *SICAX1*  
650 and used for further analysis. Sequences of evaluated genes are available in SGN Database (ITAG 2.5;  
651 <http://solgenomics.net/>). All primers used for RT-qPCR are listed in Supplemental Table S2.

652

## 653 SUPPLEMENTAL DATA

654 The following supplemental materials are available.

655 **Supplemental Table S1.** Genetic analysis of the T2 progeny of *pms916* mutant.

656 **Supplemental Table S2.** Primers used for standard and RT-qPCR analyses.

657 **Supplemental Figure S1.** Phenotype of T3 azygous (WT phenotype, left) and homozygous (*Slcbl10* mutant  
658 phenotype, right) plants for the *Slcbl10* mutation grown in absence of salt stress.

659 **Supplemental Figure S2.** The lack of *SICBL10* alters  $K^+$  content in tomato plant under salt stress.

660 **Supplemental Figure S3.**  $Na^+$  extrusion is increased in *Slcbl10* under salinity.

661 **Supplemental Figure S4.** Phenotype of *Slcbl10* tomato mutant plants salt-treated for a long time in a  
662 greenhouse.

663 **Supplemental Figure S5.** Phenotype of RNAi *SICBL10* plants salt-treated for a long time in a greenhouse.

664 **Supplemental Figure S6.** Effects of calcium deficiency on shoot apex development.

665

666 **ACKNOWLEDGMENTS:**

667 This study was supported by grants from the Plant KBBE Program (EUI2009-04074), the Spanish Ministerio de  
668 Economía y Competitividad (AGL2012-40150 and AGL2015-64991), and Seneca Foundation (18973/JLI/13),  
669 as well as the French National Research Agency ENDOREPIGEN project. A.O-A. was supported by a PhD  
670 fellowship from the Spanish Ministerio de Economía y Competitividad (BIO2009-11484).

671

672 **FIGURE LEGENDS**

673 **Figure 1.** Molecular cloning of *pms916* salt hypersensitive T-DNA mutant. (A) Phenotype of *pms916* mutant  
674 plants grown *in vitro* after 20 days of 100 mM NaCl salt treatment (DST). (B) Southern blot analysis using a  
675 chimeric probe which includes the complete coding sequence of the *NEOMICIN PHOSPHOTRANSFERASE II*  
676 (*NPTII*) gene fused to 811 pb of the coding sequence of *FALSIFLORA (FA)* gene (used as hybridization positive  
677 control). (C) Genomic organization of the *SICBL10* gene and the two T-DNA copies inserted in a head-to-tail  
678 tandem orientation in the *pms916* mutant. The tandem T-DNA insertion resulted in a 1,836 bp deletion between  
679 -1,634 and 202 bp in the *SICBL10* gene. Number 1 indicates the translation start site, and 8,766 indicates the  
680 last nucleotide of the coding region. Exons are depicted as black boxes; the lines between boxes are introns. The  
681 dotted lines indicate the position where the insertion is located. The grey arrows indicate the primers used for  
682 genotyping the T2 population. G-F and G-R: specific genomic forward and reverse primers, respectively, used  
683 to amplify the wild-type allele (without T-DNA insertion). G-F and T2-R: specific genomic forward and  
684 specific T-DNA border primers, respectively, used to amplify the mutant allele (carrying the T-DNA insertion).  
685 (D) Genotyping of T2 individuals. All T2 plants homozygous for the mutant allele (1, 5, 7, 8, 12, 13, and 15)  
686 displayed *pms916* mutant phenotype, while T2 plants heterozygous (2, 3, 4, 6, 9, 10, 11, 14, 16, 17, 18, 20, 23,  
687 and 24) and homozygous for the Wild-type allele (19, 21, 22, and 25) showed wild-type phenotype.

688

689 **Figure 2.** *SICBL10* protects the tomato shoot apex and young tissues from salt stress conditions. (A) WT and  
690 *Slcbl10* mutant plants grown in a hydroponic system and salt-treated at cotyledon development stage (HSTy  
691 assay). Framed in red a *Slcbl10* mutant plant severely damaged by salinity, particularly in the shoot apex (arrow).  
692 (B) Phenotype of adult WT and *Slcbl10* mutant plants grown in a hydroponic system and salt-treated at the 5<sup>th</sup>  
693 fully developed leaf stage (HSTa assay). Note that shoot apex and young tissues of mutant plants are severely  
694 affected by salinity while adult leaves display a similar appearance to WT (pointed with red arrows). (C)  
695 Phenotype of RNAi *SICBL10* and control plants subjected to hydroponic salt treatment (HSTa assay  
696 conditions). Note that RNAi *SICBL10* plant phenocopies the mutant phenotype under saline conditions. (D)  
697 Changes in shoot and root fresh weights of WT, *Slcbl10* mutant and RNAi *SICBL10* plants during salt  
698 treatment. Values are the mean  $\pm$  SE of two independent assays, each with three biological replicates. Asterisks  
699 indicate significant differences (Student's *t*-test,  $P < 0.05$ ).

700

701 **Figure 3.** Ectopic *SICBL10* expression restores salt tolerance in the *Arabidopsis cbl10* mutant. Five-day-old  
702 seedlings of WT (Col-0), *cbl10* mutant and three transgenic lines (L3-5) overexpressing *SICBL10* in an  
703 *Arabidopsis cbl10* mutant genetic background were transferred to MS supplemented with 100 mM NaCl. (A)  
704 Representative plants 10 days after transfer. (B) Fresh weight per seedling. Black bars, without NaCl treatment;  
705 hatched bars 100 mM NaCl treatment. (C) Sodium accumulation in plants of the indicated genotypes after 10  
706 days.

707

708 **Figure 4.** Expression pattern of *SICBL10* gene in WT plants under salt stress conditions. WT plants grown in a  
709 hydroponic system and salt-treated at the 5<sup>th</sup> fully developed leaf stage (HSTa assay). (A) Levels of *SICBL10*  
710 transcripts were quantified by RT-qPCR in apex, young leaf, upper adult leaf (1<sup>st</sup> fully developed leaf), stem (1<sup>st</sup>  
711 internode) and root of WT plants developed in absence of salt (0 DST) and after 2 days of salt treatment (2

712 DST). (B) Time-course analysis of *SlCBL10* gene expression during 6 days of salt treatment (144 h) was  
713 analysed in upper adult leaf. Values are the mean  $\pm$  SE of two independent assays, each with three biological  
714 replicates. Different lowercase letters indicate significant differences determined by ANOVA ( $P < 0.05$ ).

715

716 **Figure 5.** The salt-hypersensitivity phenotype of *Slcbl10* mutant is associated with an altered  $\text{Na}^+$  long distance  
717 distribution promoted by an impaired capacity to compartmentalize  $\text{Na}^+$  into leaf vacuole. WT and *Slcbl10*  
718 mutant plants were cultivated in a hydroponic system under salt conditions (HSTa assay). (A)  $\text{Na}^+$  content and  
719 (B)  $\text{Na}^+/\text{K}^+$  ratio were analysed in apex, upper adult leaves (1<sup>st</sup> fully developed leaf), stem (1<sup>st</sup> internode) and  
720 root after 2 and 6 days of salt treatment (DST). (C) Relative expression of key genes involved in long-distance  
721  $\text{Na}^+$  distribution (*SISOS2*, *SISOS1* and *SlHKT1;2*) and in  $\text{Na}^+$  compartmentalization into the vacuole (*SINHX3*,  
722 *SINHX4*, *SlAV1*, *SlVHA-A1*) was analysed in upper adult leaves at 0 DST and after 2 DST. Values are the mean  
723  $\pm$  SE of two independent assays, each with three biological replicates. Asterisks indicate significant differences  
724 (Student's *t*-test,  $P < 0.05$ ).

725

726 **Figure 6.** *SlCBL10* disruption promoted the retention of  $\text{Ca}^{2+}$  in leaf and stem under salinity conditions. (A) WT  
727 and *Slcbl10* mutant plants grown in a hydroponic system under salt conditions (HSTa assay).  $\text{Ca}^{2+}$  content was  
728 analysed in stem (1<sup>st</sup> internode) and in the 1<sup>st</sup> developed leaf prior to salt treatment (0 DST) and after 2 and 6  
729 DST. (B) Grafted plants between WT and *Slcbl10* mutant were subjected to hydroponic salt treatment (HSTa  
730 assay conditions).  $\text{Ca}^{2+}$  content was analysed in the 1<sup>st</sup> developed leaf and in root at 0 DST and 6 DST. (C) Fruit  
731 yield, fruit number and BER incidence in WT and mutant plants at 0 DST and after 50 DST. Values are the  
732 mean  $\pm$  SE of three biological replicates of five plants each. Asterisks indicate significant differences between  
733 WT and *Slcbl10* mutant (Student's *t*-test,  $P < 0.05$ ). Different lowercase letters indicate significant differences  
734 in each tissue (root or leaf) determined by ANOVA ( $P < 0.05$ ).

735



736 **Figure 7.** *SICBL10* disruption alters the influx and efflux of  $\text{Ca}^{2+}$  in vacuole. WT and *Slcbl10* mutant plants  
737 grown in a hydroponic system under salt conditions (HSTa assay). Relative gene expression of *SICAX1*,  
738 *SITPC1*, *SIAPV1* and *SIVHA-A1* was recorded in upper adult leaf of WT and *Slcbl10* mutant during 6 days of  
739 salt stress. Values are the mean  $\pm$  SE of two independent assays, each with three biological replicates. Asterisks  
740 indicate significant differences (Student's *t*-test,  $P < 0.05$ ).

741

742 **Figure 8.** *SICBL10* gene is involved in maintaining a suitably low  $\text{Na}^+/\text{Ca}^{2+}$  ratio in tomato apex and flower  
743 under salinity conditions. WT, *Slcbl10* mutant and RNAi *SICBL10* plants grown in a hydroponic system and  
744 salt-treated at the 5<sup>th</sup> fully developed leaf stage (HSTa assay).  $\text{Na}^+$  (A) and  $\text{Ca}^{2+}$  contents (B) were analysed in  
745 upper adult leaf, apex and flower after 6 days of salt treatment (DST), and then the  $\text{Na}^+/\text{Ca}^{2+}$  ratio was  
746 calculated (C). Values are the mean  $\pm$  SE of two independent assays, each with three biological replicates.  
747 Different lowercase letters represent significant differences ( $P > 0.05$ ) calculated by ANOVA. (D)  
748 Representative images of WT and *Slcbl10* mutant flowers after 10 DST.

749

750 **Figure 9.** Hypothetical model of the genetic and physiological mechanism proposed to explain the functional  
751 role of *SICBL10* gene in regulating  $\text{Na}^+$  and  $\text{Ca}^{2+}$  homeostasis under salt stress conditions. On the right side, it  
752 is indicated the activity of  $\text{Na}^+$  antiporters (SOS1, NHK and KKT),  $\text{Ca}^{2+}$  antiporter (CAX), the vacuolar pumps  
753 (AVP1 and V-ATPase) and the cation vacuolar channel TPC1, all of them involved in maintaining  $\text{Na}^+/\text{Ca}^{2+}$   
754 balance through the vacuolar transport. On the left side, the mechanism would be impaired due to the lack of  
755 *SICBL10* (see Discussion section for details). Red and green colours mean down-regulated and up-regulated  
756 genes under salt stress, respectively, while grey colour represents absence of gene expression changes in salinity  
757 conditions. Different lightness of red and green colours indicate different levels of gene expression in *Slcbl10*  
758 mutant (left) respect to WT plants (right) grown in salt conditions, where darker hues represent higher induction

759 (green) or inhibition (red). The names of the proteins correspond to those of *Arabidopsis thaliana*, although  
760 results provided in this work indicate that, in general terms, this mechanism could be conserved in tomato.

761

## 762 **LITERATURE CITED**

763 Albaladejo I, Meco V, Felix Plasencia F, Flores FB, Bolarin MC, Egea I (2017) Unravelling the strategies used  
764 by the wild tomato species *Solanum pennellii* to confront salt stress: From leaf anatomical adaptations to  
765 molecular responses. *Environ Exp Bot* 135: 1-12

766 Almeida P, de Boer GJ, de Boer AH (2014) Differences in shoot Na<sup>+</sup> accumulation between two tomato species  
767 are due to differences in ion affinity of HKT1;2. *Plant Physiol* 171: 438-447

768 Asins MJ, Raga V, Roca D, Belver A, Carbonell EA (2015) Genetic dissection of tomato rootstock effects on  
769 scion traits under moderate salinity. *Theor Appl Genet* 128: 667-679

770 Asins MJ, Villalta I, Aly MM, Olías R, Álvarez de Morales P, Huertas R, Li J, Jaime-Pérez N, Haro R, Raga V,  
771 et al. (2013) Two closely linked tomato HKT coding genes are positional candidates for the major tomato  
772 QTL involved in Na<sup>+</sup>/K<sup>+</sup> homeostasis. *Plant Cell Environ* 36: 1171-1191

773 Atarés A, Moyano E, Morales B, Schleicher P, García-Abellán J, Antón T, García-Sogo B, Pérez-Martín F,  
774 Lozano R, Flores FB, et al. (2011) An insertional mutagenesis programme with an enhancer trap for the  
775 identification and tagging of genes involved in abiotic stress tolerance in the tomato wild-related species  
776 *Solanum pennellii*. *Plant Cell Rep* 30: 1865-1879

777 Ausubel FM, Brent R, Kingston RE, Moore DD, Seidman JG, Smith JA, Struhl K (1993) *Current Protocols in*  
778 *Molecular Biology*, vol. 2. Wiley Interscience, New York. 2.9.1-2.9.15

779 Bageshwar UK, Taneja-Bageshwar S, Moharram HM, Binzel ML (2005) Two isoforms of the A subunit of the  
780 vacuolar H<sup>+</sup>-ATPase in *Lycopersicon esculentum*: highly similar proteins but divergent patterns of tissue  
781 localization. *Planta* 220: 632-643

782 Batelli G, Verslues PE, Agius F, Qiu Q, Fujii H, Pan S, Schumaker KS, Grillo S, Zhu JK (2007) SOS2  
783 promotes salt tolerance in part by interacting with the vacuolar H<sup>+</sup>-ATPase and upregulating its transport  
784 activity. *Mol Cell Biol* 27: 7781-7790

785 Batistic O, Waadt R, Steinhorst L, Held K, Kudla J (2010) CBL-mediated targeting of CIPKs facilitates the  
786 decoding of calcium signals emanating from distinct cellular stores. *Plant J* 61: 211-222

787 Bonales-Alatorre E, Pottosin I, Shabala L, Chen ZH, Zeng F, Jacobsen SE, Shabala S (2013) Differential  
788 activity of plasma and vacuolar membrane transporters contributes to genotypic differences in salinity  
789 tolerance in a halophyte species, *Chenopodium quinoa*. *Int J Mol Sci* 14: 9267-9285

790 Busse SB, Ozgen S, Palta JP (2008) Influence of root zone calcium on subapical necrosis in potato shoot  
791 cultures: Localization of injury at the tissue and cellular levels. *J Am Soc Hortic Sci* 133: 653-662

792 Campos JF, Cara B, Pérez-Martín F, Pineda B, Egea I, Flores FB, Fernández-García N, Capel J, Moreno V,  
793 Angosto T, et al. (2016) The tomato mutant *ars1* (*altered response to salt stress 1*) identifies an R1-type  
794 MYB transcription factor involved in stomatal closure under salt acclimation. *Plant Biotechnol J* 14:  
795 1345–1356

796 Cheng NH, Pittman JP, Barkla BJ, Shigaki T, Hirschi KD (2003) The Arabidopsis *cax1* mutant exhibits  
797 impaired ion homeostasis, development, and hormonal responses and reveals interplay among vacuolar  
798 transporters. *Plant Cell* 15: 347–364

799 Choi WG, Toyota M, Kim SH, Hilleary R, Gilroy S (2014) Salt stress-induced Ca<sup>2+</sup> waves are associated with  
800 rapid, long-distance root-to-shoot signaling in plants. *PNAS* 111: 6497-6502

801 Clough SJ, Bent AF (1998) Floral dip: a simplified method for *Agrobacterium*-mediated transformation of  
802 *Arabidopsis thaliana*. *Plant J* 16: 735-743

803 Conn SJ, Gilliam M, Athman A, Schreiber AW, Baumann U, Moller I, Cheng NH, Stancombe MA, Hirschi  
804 KD, Webb AAR, et al. (2011) Cell-specific vacuolar calcium storage mediated by CAX1 Regulates

805 apoplastic calcium concentration, gas exchange, and plant productivity in Arabidopsis. *Plant Cell* 23: 240-  
806 257

807 Cuartero J, Bolarin MC, Moreno V, Pineda B (2010) Molecular tools for enhancing salinity tolerance in plants.  
808 In SM Jain, DS Brar, eds, *Molecular techniques in crop improvement*. Springer, New York. 373-405

809 Dayod M, Tyerman SD, Leigh RA, Gilliam M (2010) Calcium storage in plants and the implications for  
810 calcium biofortification. *Protoplasma* 247: 215-231.

811 de Freitas ST, McElrone AJ, Shackel KA, Mitcham EJ (2014) Calcium partitioning and allocation and blossom-  
812 end rot development in tomato plants in response to whole-plant and fruit-specific abscisic acid  
813 treatments. *J Exp Bot* 65: 235-247

814 de la Torre F, Gutiérrez-Beltrán E, Pareja-Jaime Y, Chakravarthy S, Martin GB, del Pozo O (2013) The tomato  
815 calcium sensor CBL10 and its interacting protein kinase CIPK6 define a signaling pathway in plant  
816 immunity. *Plant Cell* 25: 2748-2764

817 Dellaporta SL, Wood J, Hicks JB (1983) A plant DNA miniprep: version II. *Plant Mol Biol Rep* 1: 19-21

818 Evans MJ, Choi WG, Gilroy S, Morris RJ (2016) A ROS-assisted calcium wave dependent on the AtRBOHD  
819 NADPH oxidase and TPC1 cation channel propagates the systemic response to salt stress. *Plant Physiol*  
820 171: 1771-84

821 Flowers TJ, Galal HK, Bromham L (2010) Evolution of halophytes: Multiple origins of salt tolerance in land  
822 plants. *Funct Plant Biol* 37: 604-612

823 Furuichi T, Cunningham KW, Muto S (2001) A putative two pore channel AtTPC1 mediates Ca<sup>2+</sup> flux in  
824 Arabidopsis leaf cells. *Plant Cell Physiol* 42: 900-5

825 Galvez FJ, Baghour M, Hao G, Cagnac O, Rodríguez-Rosales MP, Venema K (2012) Expression of *LeNHX*  
826 isoforms in response to salt stress in salt sensitive and salt tolerant tomato species. *Plant Physiol Bioch* 51:  
827 109-115

828 García-Abellan JO, Egea I, Pineda B, Sanchez-Bel P, Belver A, García-Sogo B, Flores FB, Atarés A, Moreno  
829 V, Bolarin MC (2014) Heterologous expression of the yeast *HAL5* gene in tomato enhances salt tolerance  
830 by reducing shoot  $\text{Na}^+$  accumulation in the long term. *Physiol Plantarum* 152: 700–713

831 Gaxiola RA, Palmgren MG, Schumacher K (2007) Plant proton pumps. *FEBS Lett* 581: 2204-2214

832 Gisbert C, Rus AM, Bolarin MC, Lopez-Coronado JM, Arrillaga I, Montesinos C, Caro M, Serrano R, Moreno  
833 V (2000) The yeast *HAL1* gene improves salt tolerance of transgenic tomato. *Plant Physiol* 123: 392–402

834 Gleave AP (1992) A versatile binary vector system with a T-DNA organisational structure conducive to  
835 efficient integration of cloned DNA into the plant genome. *Plant Mol Biol* 20: 1203–1207

836 Hasegawa PM (2013) Sodium ( $\text{Na}^+$ ) homeostasis and salt tolerance of plants. *Environ Exp Bot* 92: 19–31

837 Hedrich R, Marten I (2011) TPC1 – SV Channels Gain Shape. *Mol Plant* 4: 428-441

838 Hirschi K.D (1999) Expression of Arabidopsis *CAX1* in Tobacco: Altered calcium homeostasis and increased  
839 stress sensitivity. *Plant Cell* 11: 2113-2122

840 Hoagland DR Arnon DI (1950) The water-culture method for growing plants without soil. In: *Agricultural*  
841 *Experiment Station Circular 347*, Berkeley, The College of Agriculture University of California, 1–32

842 Huertas R, Rubio L, Cagnac O, García-Sánchez MJ, Alché JDD, Venema K, Fernández JA, Rodríguez-Rosales  
843 MP (2013) The  $\text{K}^+/\text{H}^+$  antiporter *LeNHX2* increases salt tolerance by improving  $\text{K}^+$  homeostasis in  
844 transgenic tomato. *Plant Cell Environ* 36: 2135-2149

845 Kang HK, Nam KH (2016) Reverse function of ROS-induced CBL10 during salt and drought stress responses.  
846 *Plant Sci* 243: 49-55

847 Kim BG, Waadt R, Cheong YH, Pandey GK, Dominguez-Solis JR, Schültke S, Lee SC, Kudla J, Luan S (2007)  
848 The calcium sensor CBL10 mediates salt tolerance by regulating ion homeostasis in Arabidopsis. *Plant J*  
849 52: 473-484

850 Kim KN (2013) Stress responses mediated by the CBL calcium sensors in plants. *Plant Biotechnol Rep* 7: 1-8

851 Kintzer AF, Stroud RM (2016) Structure, inhibition and regulation of two-pore channel TPC1 from *Arabidopsis*  
852 *thaliana*. *Nature* 531: 258-264.

853 Kolukisaoglu Ü, Weinl S, Blazevic D, Batistic O, Kudla J (2004) Calcium sensors and their interacting protein  
854 kinases: genomics of the *Arabidopsis* and rice CBL-CIPK signaling networks. *Plant Physiol* 134: 43-58

855 Lin H, Yang Y, Quan R, Mendoza I, Wu Y, Du W, Zhao S, Schumaker KS, Pardo JM, Guo Y (2009)  
856 Phosphorylation of SOS3-like calcium binding protein 8 by SOS2 protein kinase stabilizes their protein  
857 complex and regulates salt tolerance in *Arabidopsis*. *Plant Cell* 21: 1607-1619

858 Livak KJ, Schmittgen TD (2001) Analysis of relative gene expression data using real-time quantitative PCR and  
859 the 2(-Delta Delta C(T)) method. *Methods* 25: 402-408

860 Luan S (2008) The CBL-CIPK network in plant calcium signaling. *Trends Plant Sci* 14: 37-42

861 Maathuis FJM (2009) Physiological functions of mineral macronutrients. *Curr Opin Plant Biol* 12: 250-258

862 Maathuis FJM (2014) Sodium in plants: perception, signalling, and regulation of sodium fluxes. *J Exp Bot* 65:  
863 849-858

864 Maeshima M (2000) Vacuolar H<sup>+</sup>-pyrophosphatase. *Biochim Biophys Acta* 1465: 37-51

865 Manaa A, Faurobert M, Valot B, Bouchet JP, Grasselly D, Causse M, Ahmed HB (2013) Effect of salinity and  
866 calcium on tomato fruit proteome. *OMICS* 17:328-352

867 Manohar M, Shigaki T, Hirschi KD (2011) Plant cation/H<sup>+</sup> exchangers (CAXs): biological functions and  
868 genetic manipulation. *Plant Biol* 13: 561-569

869 Monihan SM, Magness CA, Yadegari R, Smith SE, Schumaker KS (2016) *Arabidopsis* CALCINEURIN B-  
870 LIKE10 functions independently of the SOS pathway during reproductive development in saline  
871 conditions. *Plant Physiol* 171: 369-379

872 Murashige T, Skoog F (1962) A revised medium for rapid growth and bio assays with Tobacco tissue cultures.  
873 *Physiol Plant* 15: 473-497

- 874 Olias R, Eljakaoui Z, Li J, de Morales PA, Marín-Manzano MC, Pardo JM, Belver A (2009) The plasma  
875 membrane Na<sup>+</sup>/H<sup>+</sup> antiporter SOS1 is essential for salt tolerance in tomato and affects the partitioning of  
876 Na<sup>+</sup> between plant organs. *Plant Cell Environ* 32: 904-916
- 877 Park S, Cheng NH, Pittman JK, Yoo KS, Park J, Smith RH, Hirschi KD (2005) Increased calcium levels and  
878 prolonged shelf life in tomatoes expressing *Arabidopsis* H<sup>+</sup>/Ca<sup>2+</sup> transporters. *Plant Physiol* 139: 1194–  
879 206
- 880 Peiter E (2011) The plant vacuole: Emitter and receiver of calcium signals. *Cell Calcium* 50: 120-128
- 881 Pérez-Martín F, Yuste-Lisbona FJ, Pineda B, Angarita-Díaz MP, García-Sogo B, Antón T, Sánchez S, Giménez  
882 E, Atarés A, Fernández-Lozano A, et al (2017) A collection of enhancer trap insertional mutants for  
883 functional genomics in tomato. *Plant Biotechnol J* 15:1439-1452
- 884 Pineda B, García–Abellán JO, Antón T, Pérez F, Moyano E, García–Sogo B, Campos JF, Angosto T, Morales  
885 B, Capel J, et al. (2012) Genomic approaches for salt and drought stress tolerance in tomato. In N Tuteja,  
886 SS Gill, AF Tiburcio, R Tuteja, eds, *Improving Crop Resistance to Abiotic Stress*. Wiley-VCH Verlag  
887 and Co. KGaA, Weinheim. 1085–1110
- 888 Pittman JK, Edmond C, Sunderland PA, Bray CM (2009) A cation-regulated and proton gradient-dependent  
889 cation transporter from *Chlamydomonas reinhardtii* has a role in calcium and sodium homeostasis. *J Biol*  
890 *Chem* 284: 525-533
- 891 Platten JD, Cotsaftis O, Berthomieu P, Bohnert H, Davenport RJ, Fairbairn DJ, Horie T, Leigh RA, Lin HX,  
892 Luan S, et al. (2006) Nomenclature for HKT transporters, key determinants of plant salinity tolerance.  
893 *Trends Plant Sci* 11: 372–374
- 894 Qiu QS, Guo Y, Quintero FJ, Pardo JM, Schumaker KS, Zhu JK (2004) Regulation of vacuolar Na<sup>+</sup>/H<sup>+</sup>  
895 exchange in *Arabidopsis thaliana* by the salt-overly-sensitive (SOS) pathway. *J Biol Chem* 279: 207–15

896 Quan R, Lin H, Mendoza I, Zhang Y, Cao W, Yang Y, Shang M, Chen S, Pardo JM, Guo Y (2007)  
897 SCABP8/CBL10, a putative calcium sensor, interacts with the protein kinase SOS2 to protect Arabidopsis  
898 shoots from salt stress. *Plant Cell* 19: 1415–31

899 Robertson D (2013) Modulating Plant Calcium for Better Nutrition and Stress Tolerance. *ISRN Botany Article*  
900 ID 952043.

901 Shabala S (2013) Learning from halophytes: physiological basis and strategies to improve abiotic stress  
902 tolerance in crops. *Ann Bot* 112: 1209–1221

903 Shabala S, Shabala L, Van Volkenburgh E, Newman I (2005) Effect of divalent cations on ion fluxes and leaf  
904 photochemistry in salinized barley leaves. *J Exp Bot* 56: 1369–78

905 Tang RJ, Yang Y, Yang L, Liu H, Wang CT, Yu MM, Gao XS, Zhang HX (2014) Poplar calcineurin B-like  
906 proteins PtCBL10A and PtCBL10B regulate shoot salt tolerance through interaction with PtSOS2 in the  
907 vacuolar membrane. *Plant Cell Environ* 37: 573–88

908 Uozumi A, Ikeda H, Hiraga M, Kanno H, Nanzyo M, Nishiyama M, Kanayama Y (2012) Tolerance to salt  
909 stress and blossom-end rot in an introgression line, IL8-3, of tomato. *Sci Hortic* 138: 1-6

910 Villalta I, Reina-Sánchez A, Bolarín MC, Cuartero J, Belver A, Venema K, Carbonell EA, Asins MJ (2008)  
911 Genetic analysis of Na<sup>+</sup> and K<sup>+</sup> concentrations in leaf and stem as physiological components of salt  
912 tolerance in Tomato. *Theor Appl Genet* 116: 869-80

913 Waadt R, Schmidt LK, Lohse M, Hashimoto K, Bock R, Kudla J (2008) Multicolor bimolecular fluorescence  
914 complementation reveals simultaneous formation of alternative CBL/CIPK complexes in planta. *Plant J*  
915 56: 505–16

916 Wesley SV, Helliwell CA, Smith NA, Wang M, Rouse DT, Liu Q, Gooding PS, Singh SP, Abbott D,  
917 Stoutjesdijk PA, et al. (2001) Construct design for efficient, effective and high-throughput gene silencing  
918 in plants. *Plant J* 27: 581–590



- 919 White PJ, Broadley MR (2003) Calcium in plants. *Ann Bot–Lond* 92: 487–511
- 920 Yuste–Lisbona FJ, Quinet M, Fernández–Lozano A, Pineda B, Moreno V, Angosto T, Lozano R (2016)  
921 Characterization of *vegetative inflorescence (mc–vin)* mutant provides new insight into the role of  
922 *MACROCALYX* in regulating inflorescence development of tomato. *Sci Reps* 6: 18796
- 923 Zhai Y, Yang Q, Hou M (2015) The effects of saline water drip irrigation on tomato yield, quality, and  
924 blossom–end rot incidence – A 3a Case study in the South of China. *PLoS One* 10: e0142204

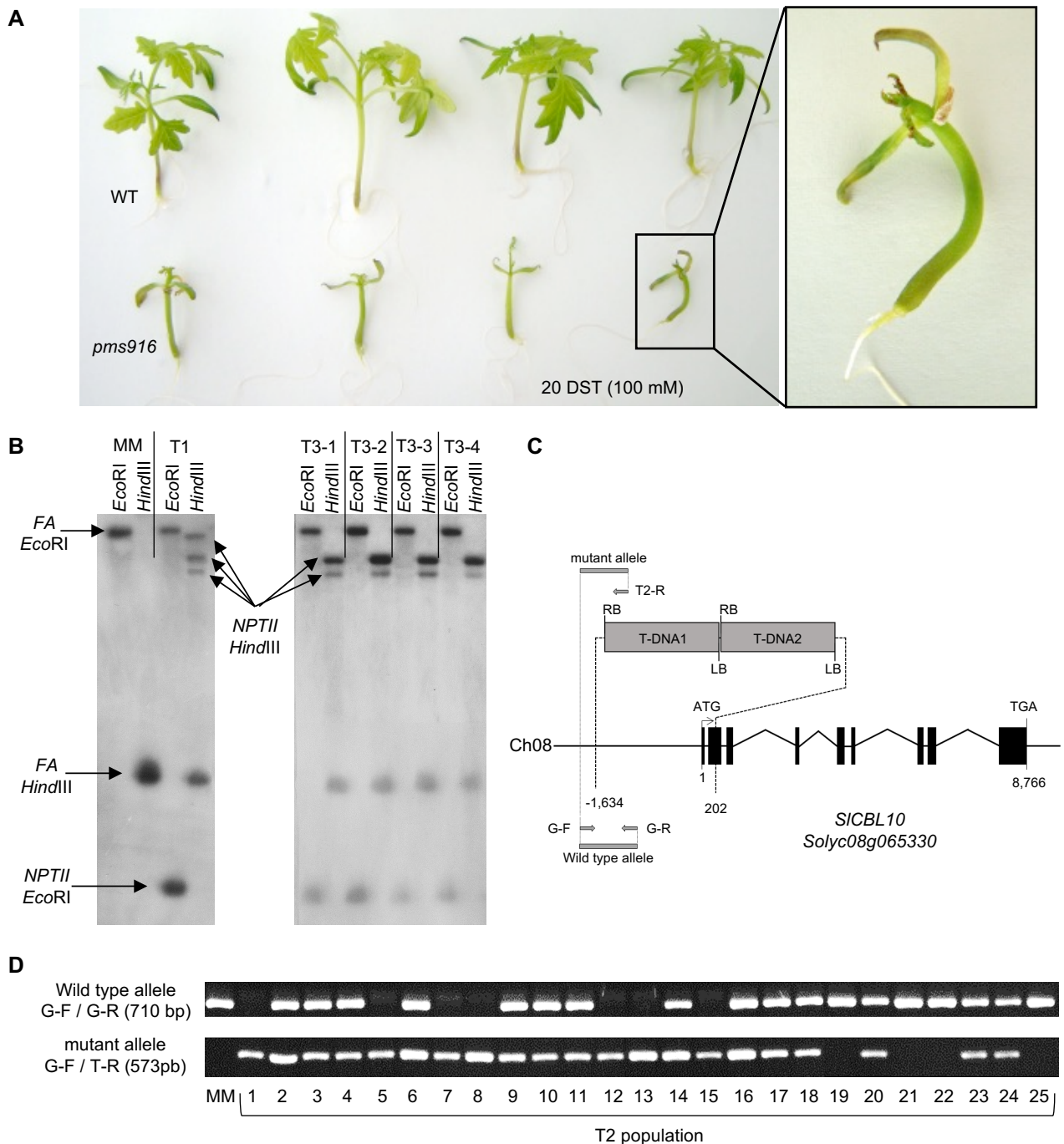


**Figure 1.** Molecular cloning of *pms916* salt hypersensitive T-DNA mutant. (A) Phenotype of *pms916* mutant plants grown *in vitro* after 20 days of 100 mM NaCl salt treatment (DST). (B) Southern blot analysis using a chimeric probe which includes the complete coding sequence of the *NEOMICIN PHOSPHOTRANSFERASE II* (*NPTII*) gene fused to 811 pb of the coding sequence of *FALSIFLORA* (*FA*) gene (used as hybridization positive control). (C) Genomic organization of the *SICBL10* gene and the two T-DNA copies inserted in a head-to-tail tandem orientation in the *pms916* mutant. The tandem T-DNA insertion resulted in a 1,836 bp deletion between  $-1,634$  and 202 bp in the *SICBL10* gene. Number 1 indicates the translation start site, and 8,766 indicates the last nucleotide of the coding region. Exons are depicted as black boxes; the lines between boxes are introns. The dotted lines indicate the position where the insertion is located. The grey arrows indicate the primers used for genotyping the T2 population. G-F and G-R: specific genomic forward and reverse primers, respectively, used to amplify the wild-type allele (without T-DNA insertion). G-F and T2-R: specific genomic forward and specific T-DNA border primers, respectively, used to amplify the mutant allele (carrying the T-DNA insertion). (D) Genotyping of T2 individuals. All T2 plants homozygous for the mutant allele (1, 5, 7, 8, 12, 13, and 15) displayed *pms916* mutant phenotype, while T2 plants heterozygous (2, 3, 4, 6, 9, 10, 11, 14, 16, 17, 18, 20, 23, and 24) and homozygous for the Wild-type allele (19, 21, 22, 23, and 24) displayed wild-type phenotype.

Downloaded from www.plantphysiol.org on December 13, 2017. Published by www.plantphysiol.org  
Copyright © 2017 American Society of Plant Biologists. All rights reserved.

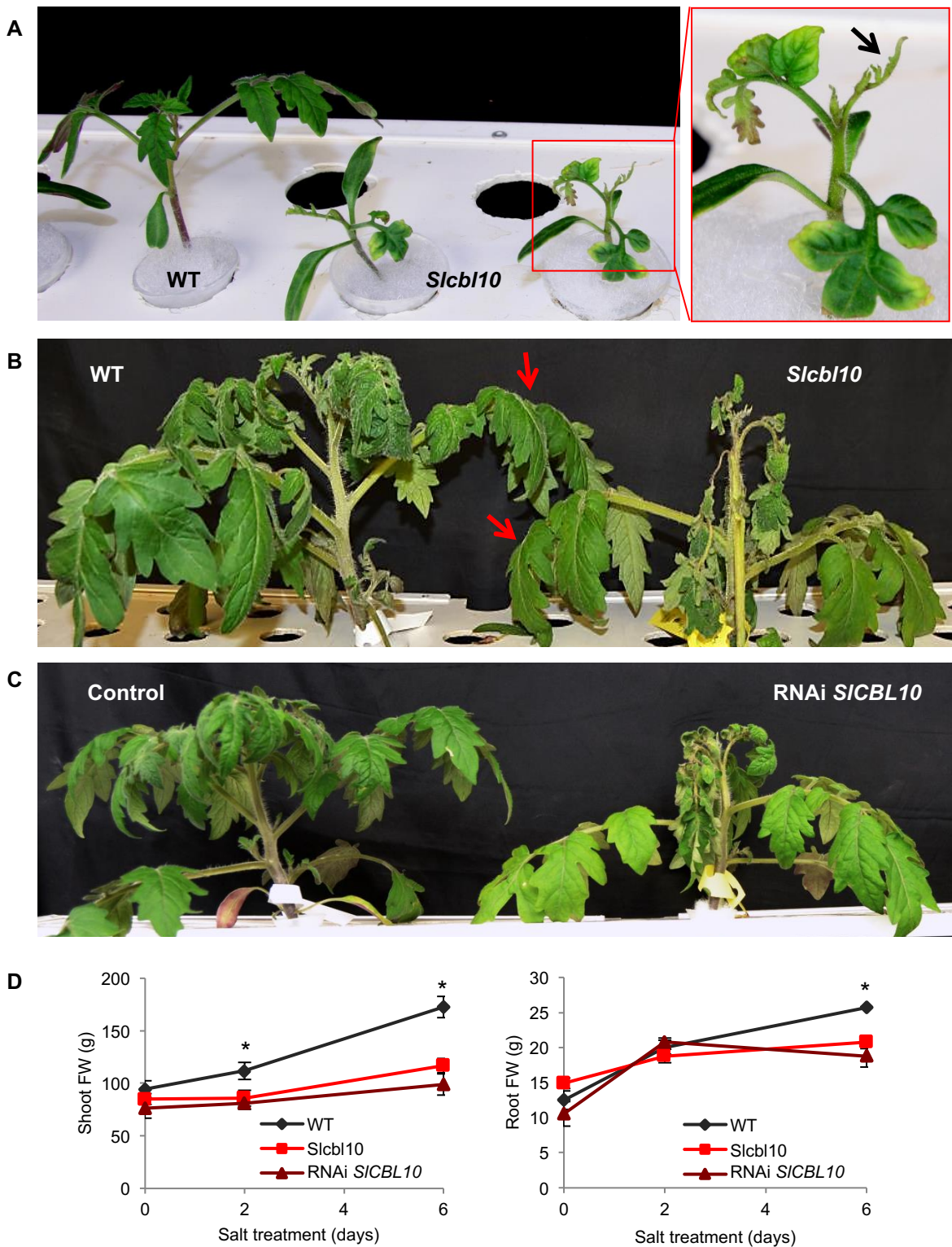


**Figure 2.** *SICBL10* protects the tomato shoot apex and young tissues from salt stress conditions. (A) WT and *Slcbl10* mutant plants grown in a hydroponic system and salt-treated at cotyledon development stage (HSTy assay). Framed in red a *Slcbl10* mutant plant severely damaged by salinity, particularly in the shoot apex (arrow). (B) Phenotype of adult WT and *Slcbl10* mutant plants grown in a hydroponic system and salt-treated at the 5<sup>th</sup> fully developed leaf stage (HSTa assay). Note that shoot apex and young tissues of mutant plants are severely affected by salinity while adult leaves display a similar appearance to WT (pointed with red arrows). (C) Phenotype of RNAi *SICBL10* and control plants subjected to hydroponic salt treatment (HSTa assay conditions). Note that RNAi *SICBL10* plant phenocopies the mutant phenotype under saline conditions. (D) Changes in shoot and root fresh weights of WT, *Slcbl10* mutant and RNAi *SICBL10* plants during salt treatment. Values are the mean  $\pm$  SE of two independent assays, each with three biological replicates. Asterisks indicate significant differences (Student's *t*-test,  $P < 0.05$ ).

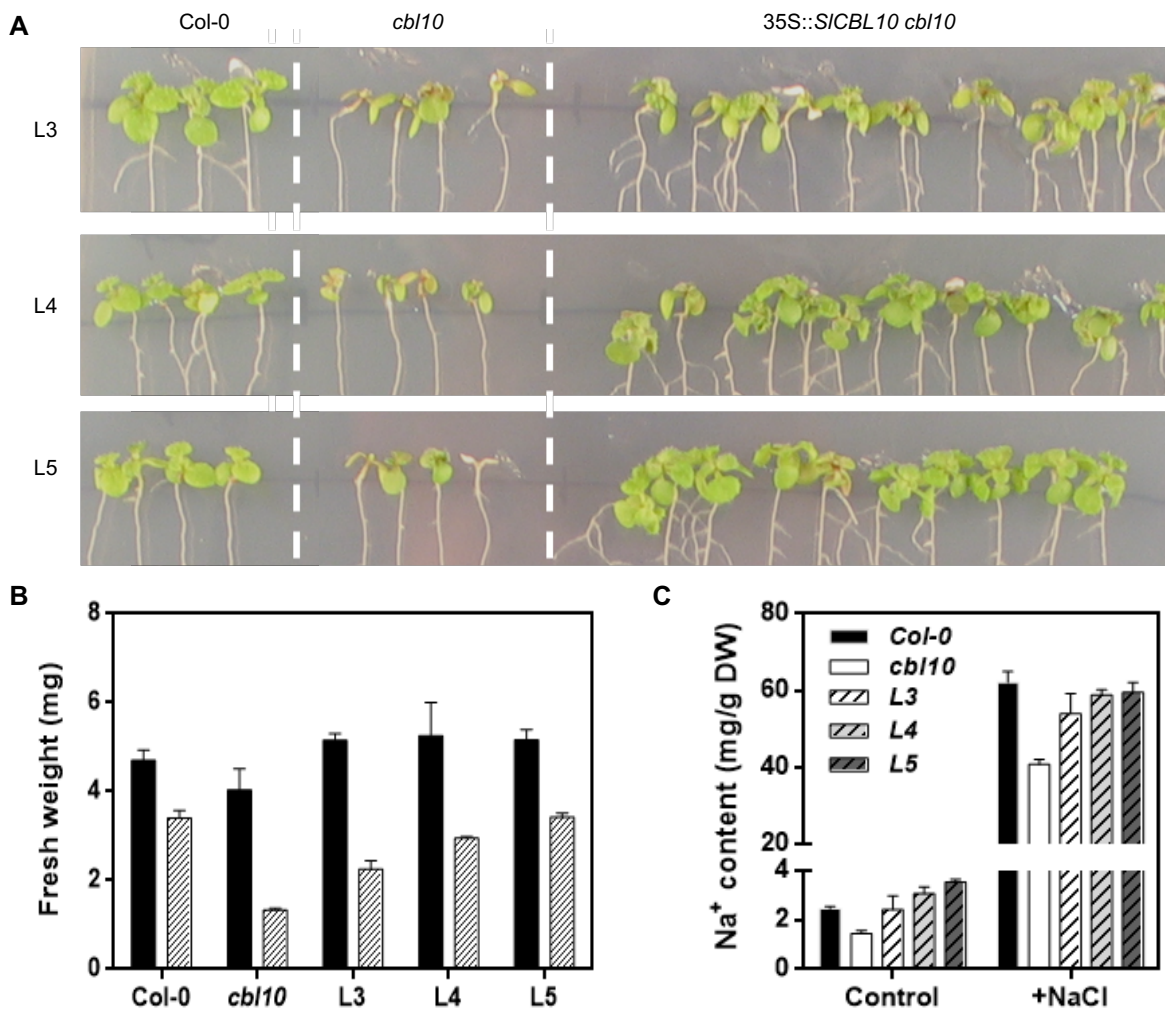


**Figure 3.** Ectopic *SICBL10* expression restores salt tolerance in the *Arabidopsis cbi10* mutant. Five-day-old seedlings of WT (Col-0), *cbi10* mutant and three transgenic lines (L3-5) overexpressing *SICBL10* in an *Arabidopsis cbi10* mutant genetic background were transferred to MS supplemented with 100 mM NaCl. (A) Representative plants 10 days after transfer. (B) Fresh weight per seedling. Black bars, without NaCl treatment; hatched bars 100 mM NaCl treatment. (C) Sodium accumulation in plants of the indicated genotypes after 10 days.

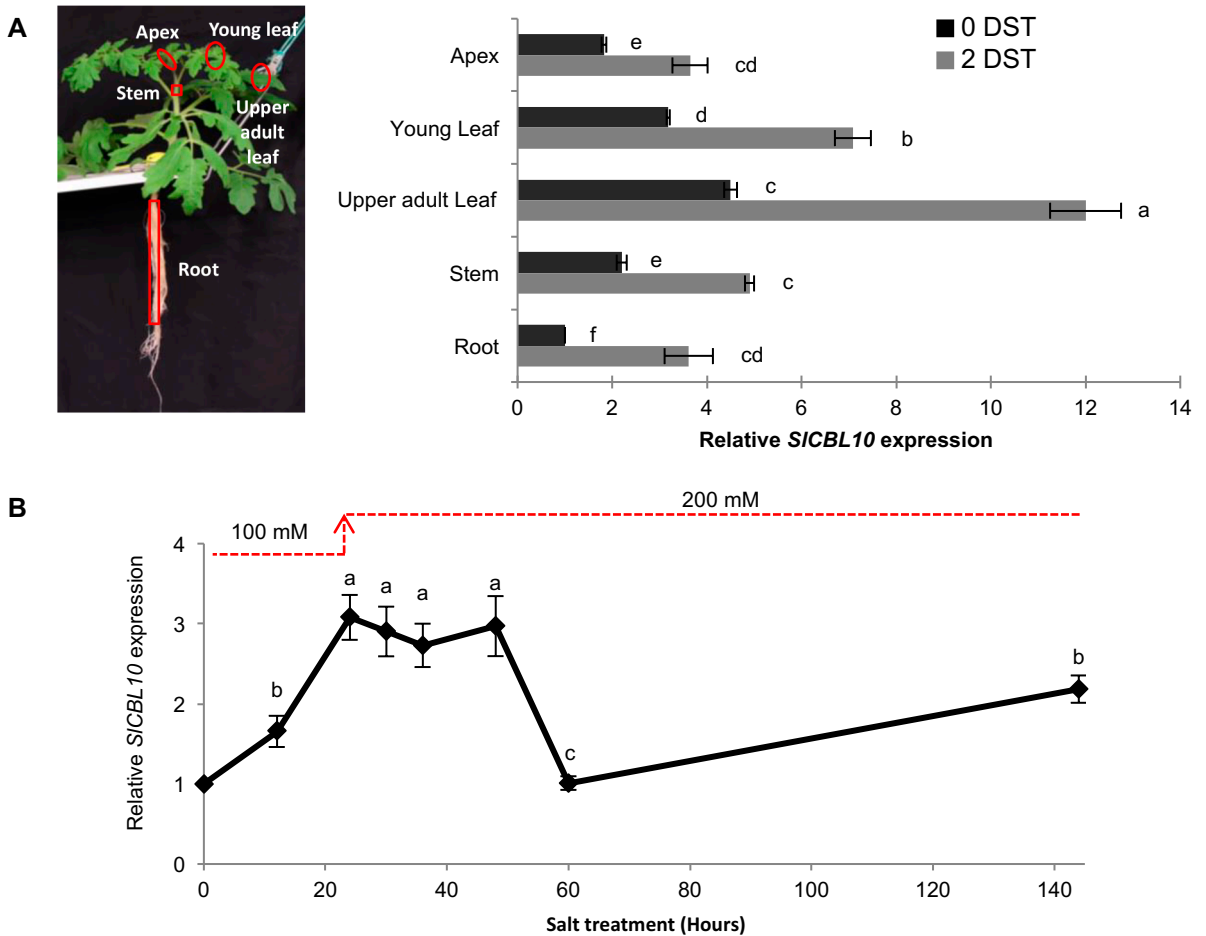


**Figure 4.** Expression pattern of *SICBL10* gene in WT plants under salt stress conditions. WT plants grown in a hydroponic system and salt-treated at the 5<sup>th</sup> fully developed leaf stage (HSTa assay). (A) Levels of *SICBL10* transcripts were quantified by RT-qPCR in apex, young leaf, upper adult leaf (1<sup>st</sup> fully developed leaf), stem (1<sup>st</sup> internode) and root of WT plants developed in absence of salt (0 DST) and after 2 days of salt treatment (2 DST). (B) Time-course analysis of *SICBL10* gene expression during 6 days of salt treatment (144 h) was analysed in upper adult leaf. Values are the mean  $\pm$  SE of two independent assays, each with three biological replicates. Different lowercase letters indicate significant differences determined by ANOVA ( $P < 0.05$ ).

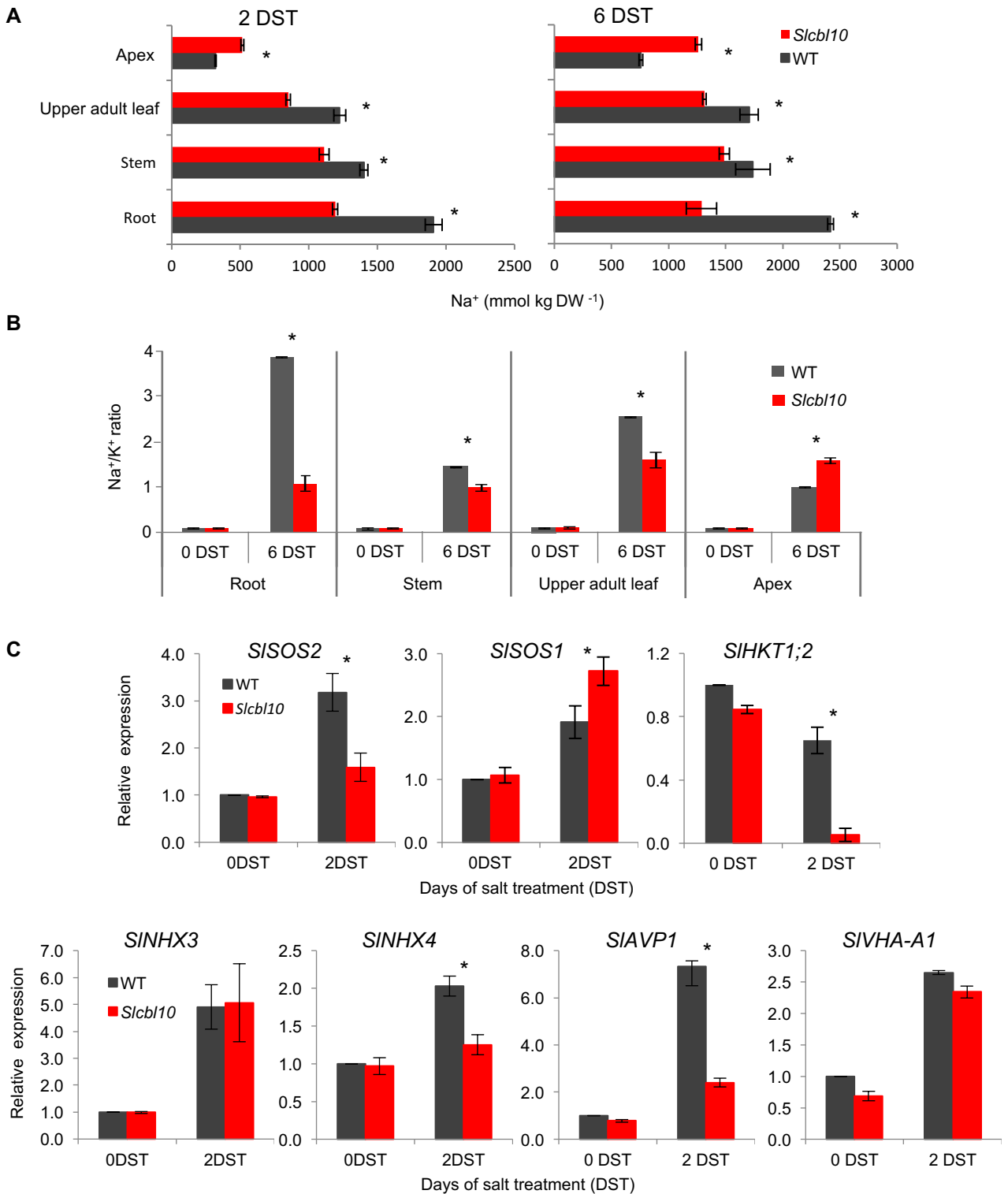


**Figure 5.** The salt-hypersensitivity phenotype of *Slcbl10* mutant is associated with an altered Na<sup>+</sup> long distance distribution promoted by an impaired capacity to compartmentalize Na<sup>+</sup> into leaf vacuole. WT and *Slcbl10* mutant plants were cultivated in a hydroponic system under salt conditions (HSTa assay). (A) Na<sup>+</sup> content and (B) Na<sup>+</sup>/K<sup>+</sup> ratio were analysed in apex, upper adult leaves (1<sup>st</sup> fully developed leaf), stem (1<sup>st</sup> internode) and root after 2 and 6 days of salt treatment (DST). (C) Relative expression of key genes involved in long-distance Na<sup>+</sup> distribution (*SISOS2*, *SISOS1* and *SIHKT1;2*) and in Na<sup>+</sup> compartmentalization into the vacuole (*SINHX3*, *SINHX4*, *SIAPV1*, *SIVHA-A1*) was analysed in upper adult leaves at 0 DST and after 2 DST. Values are the mean ± SE of two independent assays, each with three biological replicates. Asterisks indicate significant differences (Student's *t*-test, *P* < 0.05).

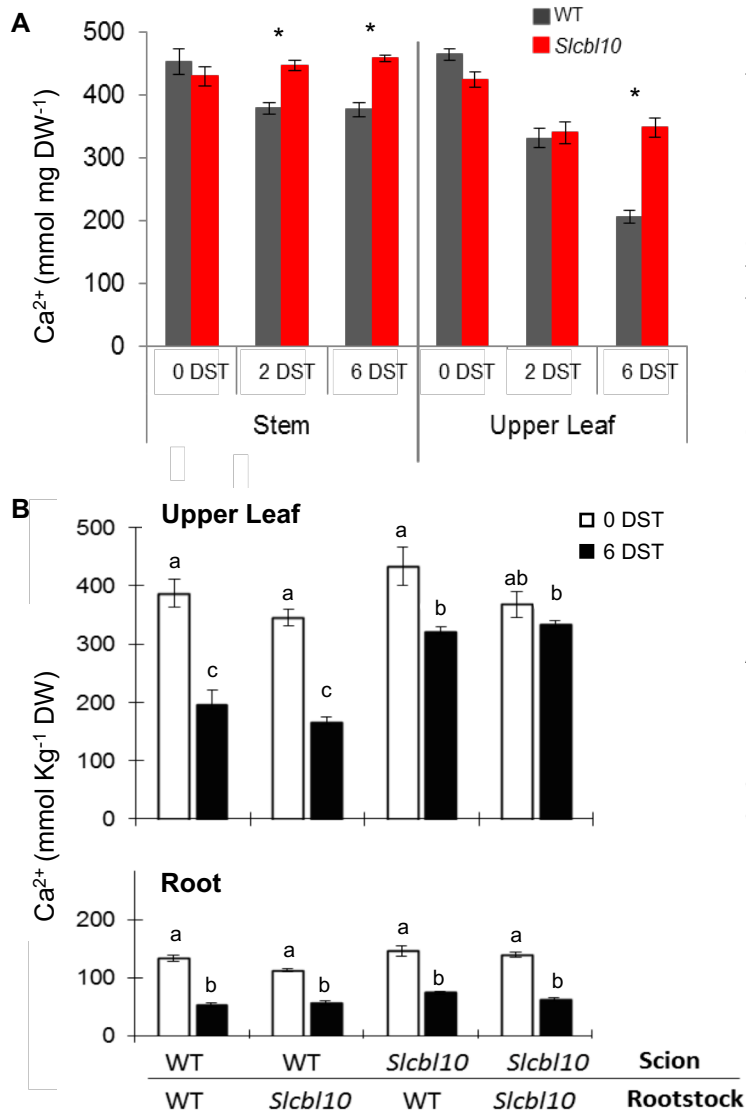


**Figure 6.** *SICBL10* disruption promoted the retention of  $\text{Ca}^{2+}$  in leaf and stem under salinity conditions. (A) WT and *Slcbl10* mutant plants grown in a hydroponic system under salt conditions (HSTa assay).  $\text{Ca}^{2+}$  content was analysed in stem (1<sup>st</sup> internode) and in the 1<sup>st</sup> developed leaf prior to salt treatment (0 DST) and after 2 and 6 DST. (B) Grafted plants between WT and *Slcbl10* mutant were subjected to hydroponic salt treatment (HSTa assay conditions).  $\text{Ca}^{2+}$  content was analysed in the 1<sup>st</sup> developed leaf and in root at 0 DST and 6 DST. (C) Fruit yield, fruit number and BER incidence in WT and mutant plants at 0 DST and after 50 DST. Values are the mean  $\pm$  SE of three biological replicates of five plants each. Asterisks indicate significant differences between WT and *Slcbl10* mutant (Student's *t*-test,  $P < 0.05$ ). Different lowercase letters indicate significant differences in each tissue (root or leaf) determined by ANOVA ( $P < 0.05$ ).

		Fruit yield (g)	Fruit number	BER (%)
0 DST	WT	1057.0 $\pm$ 132.4	43.4 $\pm$ 3.3	1.1 $\pm$ 0.3
	<i>Slcbl10</i>	399.1 $\pm$ 103.5 *	26.2 $\pm$ 4.1 *	10.2 $\pm$ 0.2 *
50 DST	WT	376.6 $\pm$ 55.2	40.2 $\pm$ 5.2	3.0 $\pm$ 0.4
	<i>Slcbl10</i>	9.9 $\pm$ 4.0 *	6.4 $\pm$ 1.8 *	70.1 $\pm$ 3.3 *



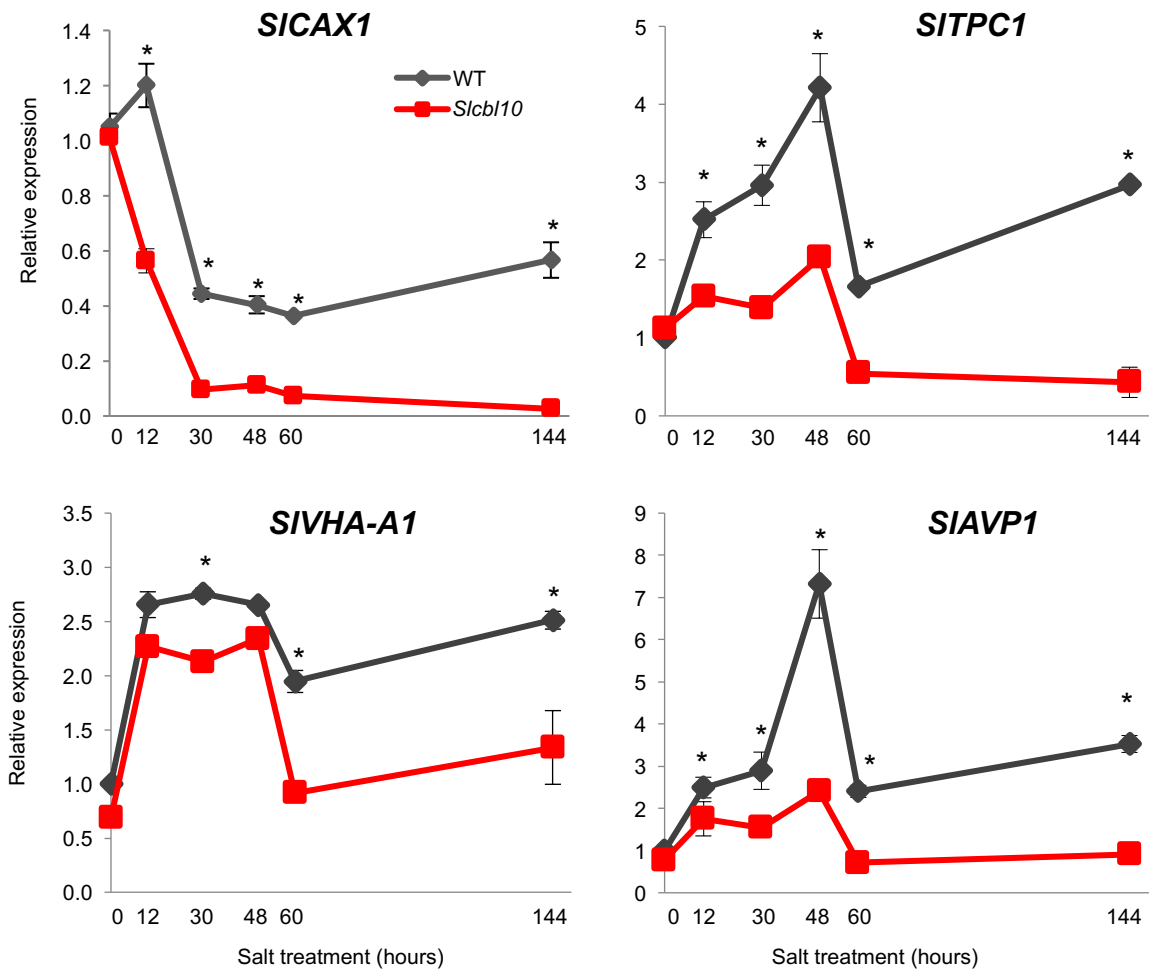


**Figure 7.** *SICBL10* disruption alters the influx and efflux of  $\text{Ca}^{2+}$  in vacuole. WT and *Slcbl10* mutant plants grown in a hydroponic system under salt conditions (HSTa assay). Relative gene expression of *SICAX1*, *SITPC1*, *SIAMP1* and *SIVHA-A1* was recorded in upper adult leaf of WT and *Slcbl10* mutant during 6 days of salt stress. Values are the mean  $\pm$  SE of two independent assays, each with three biological replicates. Asterisks indicate significant differences (Student's *t*-test,  $P < 0.05$ ).



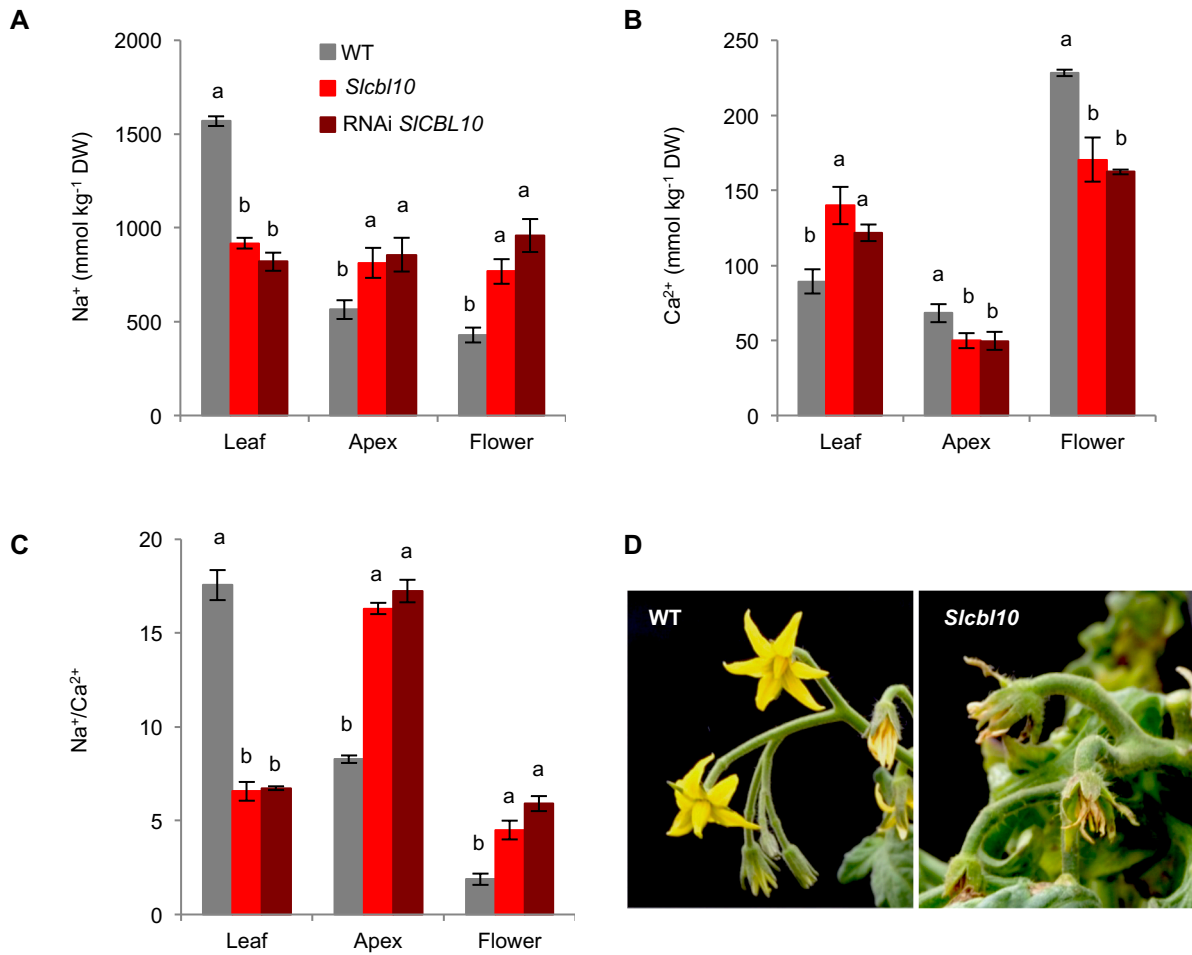


**Figure 8.** *SICBL10* gene is involved in maintaining a suitably low Na<sup>+</sup>/Ca<sup>2+</sup> ratio in tomato apex and flower under salinity conditions. WT, *Slcbl10* mutant and RNAi *SICBL10* plants grown in a hydroponic system and salt-treated at the 5<sup>th</sup> fully developed leaf stage (HSTa assay). Na<sup>+</sup> (A) and Ca<sup>2+</sup> contents (B) were analysed in upper adult leaf, apex and flower after 6 days of salt treatment (DST), and then the Na<sup>+</sup>/Ca<sup>2+</sup> ratio was calculated (C). Values are the mean ± SE of two independent assays, each with three biological replicates. Different lowercase letters represent significant differences ( $P > 0.05$ ) calculated by ANOVA. (D) Representative images of WT and *Slcbl10* mutant flowers after 10 DST.

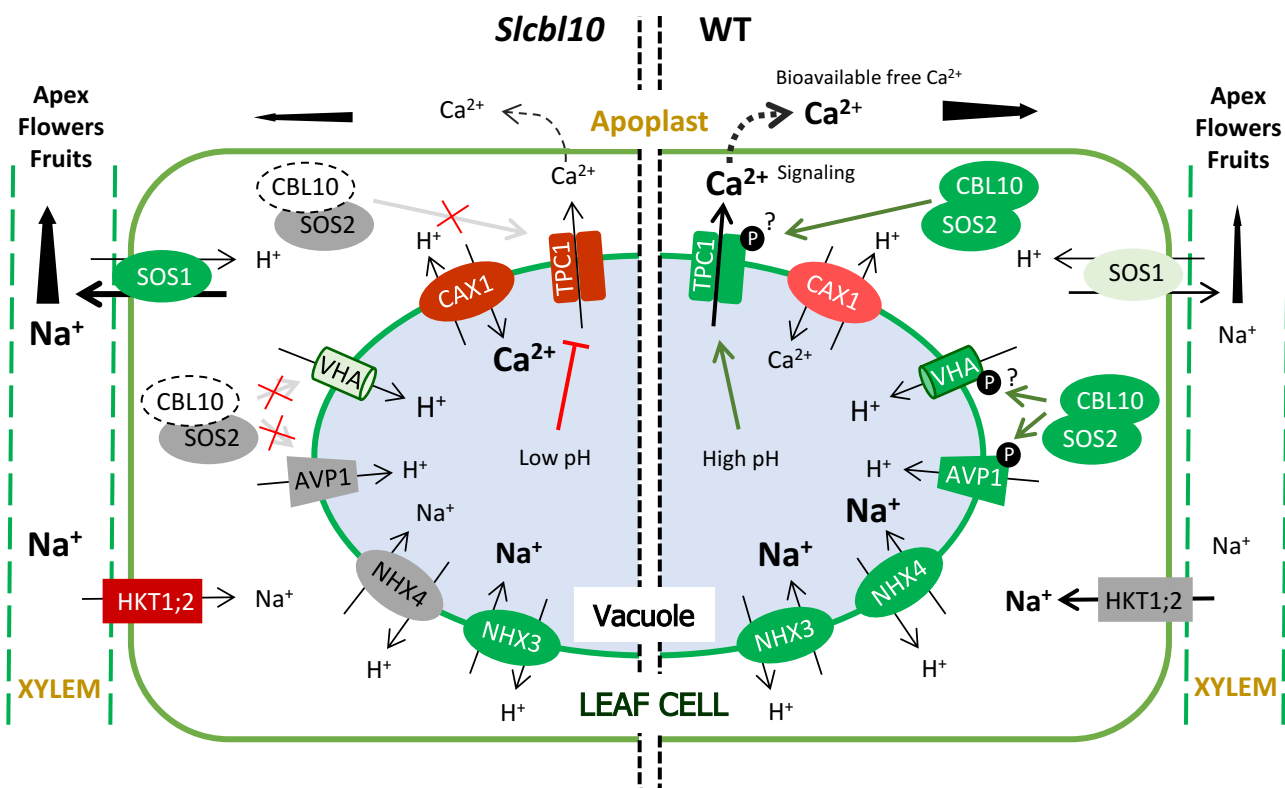


**Figure 9.** Hypothetical model of the genetic and physiological mechanism proposed to explain the functional role of *SICBL10* gene in regulating  $\text{Na}^+$  and  $\text{Ca}^{2+}$  homeostasis under salt stress conditions. On the right side, it is indicated the activity of  $\text{Na}^+$  antiporters (SOS1, NHK and KKT),  $\text{Ca}^{2+}$  antiporter (CAX), the vacuolar pumps (AVP1 and V-ATPase) and the cation vacuolar channel TPC1, all of them involved in maintaining  $\text{Na}^+/\text{Ca}^{2+}$  balance through the vacuolar transport. On the left side, the mechanism would be impaired due to the lack of *SICBL10* (see Discussion section for details). Red and green colours mean down-regulated and up-regulated genes under salt stress, respectively, while grey colour represents absence of gene expression changes in salinity conditions. Different lightness of red and green colours indicate different levels of gene expression in *Slcbl10* mutant (left) respect to WT plants (right) grown in salt conditions, where darker hues represent higher induction (green) or inhibition (red). The names of the proteins correspond to those of *Arabidopsis thaliana*, although results provided in this work indicate that, in general terms, this mechanism could be conserved in tomato.

## Parsed Citations

- Albaladejo I, Meco V, Felix Plasencia F, Flores FB, Bolarin MC, Egea I (2017) Unravelling the strategies used by the wild tomato species *Solanum pennellii* to confront salt stress: From leaf anatomical adaptations to molecular responses. *Environ Exp Bot* 135: 1-12**  
Pubmed: [Author and Title](#)  
CrossRef: [Author and Title](#)  
Google Scholar: [Author Only](#) [Title Only](#) [Author and Title](#)
- Almeida P, de Boer GJ, de Boer AH (2014) Differences in shoot Na<sup>+</sup> accumulation between two tomato species are due to differences in ion affinity of HKT1;2. *Plant Physiol* 171: 438-447**  
Pubmed: [Author and Title](#)  
CrossRef: [Author and Title](#)  
Google Scholar: [Author Only](#) [Title Only](#) [Author and Title](#)
- Asins MJ, Raga V, Roca D, Belver A, Carbonell EA (2015) Genetic dissection of tomato rootstock effects on scion traits under moderate salinity. *Theor Appl Genet* 128: 667-679**  
Pubmed: [Author and Title](#)  
CrossRef: [Author and Title](#)  
Google Scholar: [Author Only](#) [Title Only](#) [Author and Title](#)
- Asins MJ, Villalta I, Aly MM, Olías R, Álvarez de Morales P, Huertas R, Li J, Jaime-Pérez N, Haro R, Raga V, et al. (2013) Two closely linked tomato HKT coding genes are positional candidates for the major tomato QTL involved in Na<sup>+</sup>/K<sup>+</sup> homeostasis. *Plant Cell Environ* 36: 1171-1191**  
Pubmed: [Author and Title](#)  
CrossRef: [Author and Title](#)  
Google Scholar: [Author Only](#) [Title Only](#) [Author and Title](#)
- Atarés A, Moyano E, Morales B, Schleicher P, García-Abellán J, Antón T, García-Sogo B, Pérez-Martín F, Lozano R, Flores FB, et al. (2011) An insertional mutagenesis programme with an enhancer trap for the identification and tagging of genes involved in abiotic stress tolerance in the tomato wild-related species *Solanum pennellii*. *Plant Cell Rep* 30: 1865-1879**  
Pubmed: [Author and Title](#)  
CrossRef: [Author and Title](#)  
Google Scholar: [Author Only](#) [Title Only](#) [Author and Title](#)
- Ausubel FM, Brent R, Kingston RE, Moore DD, Seidman JG, Smith JA, Struhl K (1993) *Current Protocols in Molecular Biology*, vol. 2. Wiley Interscience, New York. 2.9.1-2.9.15**  
Pubmed: [Author and Title](#)  
CrossRef: [Author and Title](#)  
Google Scholar: [Author Only](#) [Title Only](#) [Author and Title](#)
- Bageshwar UK, Taneja-Bageshwar S, Moharram HM, Binzel ML (2005) Two isoforms of the A subunit of the vacuolar H<sup>+</sup>-ATPase in *Lycopersicon esculentum*: highly similar proteins but divergent patterns of tissue localization. *Planta* 220: 632-643**  
Pubmed: [Author and Title](#)  
CrossRef: [Author and Title](#)  
Google Scholar: [Author Only](#) [Title Only](#) [Author and Title](#)
- Batelli G, Verslues PE, Agius F, Qiu Q, Fujii H, Pan S, Schumaker KS, Grillo S, Zhu JK (2007) SOS2 promotes salt tolerance in part by interacting with the vacuolar H<sup>+</sup>-ATPase and upregulating its transport activity. *Mol Cell Biol* 27: 7781-7790**  
Pubmed: [Author and Title](#)  
CrossRef: [Author and Title](#)  
Google Scholar: [Author Only](#) [Title Only](#) [Author and Title](#)
- Batistic O, Waadt R, Steinhorst L, Held K, Kudla J (2010) CBL-mediated targeting of CIPKs facilitates the decoding of calcium signals emanating from distinct cellular stores. *Plant J* 61: 211-222**  
Pubmed: [Author and Title](#)  
CrossRef: [Author and Title](#)  
Google Scholar: [Author Only](#) [Title Only](#) [Author and Title](#)
- Bonales-Alatorre E, Pottosin I, Shabala L, Chen ZH, Zeng F, Jacobsen SE, Shabala S (2013) Differential activity of plasma and vacuolar membrane transporters contributes to genotypic differences in salinity tolerance in a halophyte species, *Chenopodium quinoa*. *Int J Mol Sci* 14: 9267-9285**  
Pubmed: [Author and Title](#)  
CrossRef: [Author and Title](#)  
Google Scholar: [Author Only](#) [Title Only](#) [Author and Title](#)
- Busse SB, Ozgen S, Palta JP (2008) Influence of root zone calcium on subapical necrosis in potato shoot cultures: Localization of injury at the tissue and cellular levels. *J Am Soc Hortic Sci* 133: 653-662**  
Pubmed: [Author and Title](#)  
CrossRef: [Author and Title](#)  
Google Scholar: [Author Only](#) [Title Only](#) [Author and Title](#)
- Campos JF, Cara B, Pérez-Martín F, Pineda B, Egea I, Flores FB, Fernández-García N, Capel J, Moreno V, Angosto T, et al. (2016) The tomato mutant *ars1* (altered response to salt stress 1) identifies an R1-type MYB transcription factor involved in stomatal closure under salt acclimation. *Plant Biotechnol J* 14: 1345-1356**

Pubmed: [Author and Title](#)  
CrossRef: [Author and Title](#)  
Google Scholar: [Author Only](#) [Title Only](#) [Author and Title](#)

**Cheng NH, Pittman JP, Barkla BJ, Shigaki T, Hirschi KD (2003) The Arabidopsis *cax1* mutant exhibits impaired ion homeostasis, development, and hormonal responses and reveals interplay among vacuolar transporters. Plant Cell 15: 347–364**

Pubmed: [Author and Title](#)  
CrossRef: [Author and Title](#)  
Google Scholar: [Author Only](#) [Title Only](#) [Author and Title](#)

**Choi WG, Toyota M, Kim SH, Hilleary R, Gilroy S (2014) Salt stress-induced Ca<sup>2+</sup> waves are associated with rapid, long-distance root-to-shoot signaling in plants. PNAS 111: 6497-6502**

Pubmed: [Author and Title](#)  
CrossRef: [Author and Title](#)  
Google Scholar: [Author Only](#) [Title Only](#) [Author and Title](#)

**Clough SJ, Bent AF (1998) Floral dip: a simplified method for Agrobacterium-mediated transformation of Arabidopsis thaliana. Plant J 16: 735-743**

Pubmed: [Author and Title](#)  
CrossRef: [Author and Title](#)  
Google Scholar: [Author Only](#) [Title Only](#) [Author and Title](#)

**Conn SJ, Gilliham M, Athman A, Schreiber AW, Baumann U, Moller I, Cheng NH, Stancombe MA, Hirschi KD, Webb AAR, et al. (2011) Cell-specific vacuolar calcium storage mediated by CAX1 Regulates apoplastic calcium concentration, gas exchange, and plant productivity in Arabidopsis. Plant Cell 23: 240-257**

Pubmed: [Author and Title](#)  
CrossRef: [Author and Title](#)  
Google Scholar: [Author Only](#) [Title Only](#) [Author and Title](#)

**Cuartero J, Bolarin MC, Moreno V, Pineda B (2010) Molecular tools for enhancing salinity tolerance in plants. In SM Jain, DS Brar, eds, Molecular techniques in crop improvement. Springer, New York. 373-405**

Pubmed: [Author and Title](#)  
CrossRef: [Author and Title](#)  
Google Scholar: [Author Only](#) [Title Only](#) [Author and Title](#)

**Dayod M, Tyerman SD, Leigh RA, Gilliham M (2010) Calcium storage in plants and the implications for calcium biofortification. Protoplasma 247: 215-231.**

Pubmed: [Author and Title](#)  
CrossRef: [Author and Title](#)  
Google Scholar: [Author Only](#) [Title Only](#) [Author and Title](#)

**de Freitas ST, McElrone AJ, Shackel KA, Mitcham EJ (2014) Calcium partitioning and allocation and blossom-end rot development in tomato plants in response to whole-plant and fruit-specific abscisic acid treatments. J Exp Bot 65: 235-247**

Pubmed: [Author and Title](#)  
CrossRef: [Author and Title](#)  
Google Scholar: [Author Only](#) [Title Only](#) [Author and Title](#)

**de la Torre F, Gutiérrez-Beltrán E, Pareja-Jaime Y, Chakravarthy S, Martin GB, del Pozo O (2013) The tomato calcium sensor CBL10 and its interacting protein kinase CIPK6 define a signaling pathway in plant immunity. Plant Cell 25: 2748-2764**

Pubmed: [Author and Title](#)  
CrossRef: [Author and Title](#)  
Google Scholar: [Author Only](#) [Title Only](#) [Author and Title](#)

**Dellaporta SL, Wood J, Hicks JB (1983) A plant DNA miniprep: version II. Plant Mol Biol Rep 1: 19-21**

Pubmed: [Author and Title](#)  
CrossRef: [Author and Title](#)  
Google Scholar: [Author Only](#) [Title Only](#) [Author and Title](#)

**Evans MJ, Choi WG, Gilroy S, Morris RJ (2016) A ROS-assisted calcium wave dependent on the AtRBOHD NADPH oxidase and TPC1 cation channel propagates the systemic response to salt stress. Plant Physiol 171: 1771-84**

Pubmed: [Author and Title](#)  
CrossRef: [Author and Title](#)  
Google Scholar: [Author Only](#) [Title Only](#) [Author and Title](#)

**Flowers TJ, Galal HK, Bromham L (2010) Evolution of halophytes: Multiple origins of salt tolerance in land plants. Funct Plant Biol 37: 604-612**

Pubmed: [Author and Title](#)  
CrossRef: [Author and Title](#)  
Google Scholar: [Author Only](#) [Title Only](#) [Author and Title](#)

**Furuichi T, Cunningham KW, Muto S (2001) A putative two pore channel AtTPC1 mediates Ca<sup>2+</sup> flux in Arabidopsis leaf cells. Plant Cell Physiol 42: 900-5**

Pubmed: [Author and Title](#)  
CrossRef: [Author and Title](#)  
Google Scholar: [Author Only](#) [Title Only](#) [Author and Title](#)

**Galvez FJ, Baghour M, Hao G, Cagnac O, Rodríguez–Rosales MP, Venema K (2012) Expression of LeNHX isoforms in response to salt stress in salt sensitive and salt tolerant tomato species. *Plant Physiol Bioch* 51: 109-115**

Pubmed: [Author and Title](#)

CrossRef: [Author and Title](#)

Google Scholar: [Author Only](#) [Title Only](#) [Author and Title](#)

**García-Abellan JO, Egea I, Pineda B, Sanchez–Bel P, Belder A, García-Sogo B, Flores FB, Atarés A, Moreno V, Bolarin MC (2014) Heterologous expression of the yeast HAL5 gene in tomato enhances salt tolerance by reducing shoot Na<sup>+</sup> accumulation in the long term. *Physiol Plantarum* 152: 700–713**

Pubmed: [Author and Title](#)

CrossRef: [Author and Title](#)

Google Scholar: [Author Only](#) [Title Only](#) [Author and Title](#)

**Gaxiola RA, Palmgren MG, Schumacher K (2007) Plant proton pumps. *FEBS Lett* 581: 2204-2214**

Pubmed: [Author and Title](#)

CrossRef: [Author and Title](#)

Google Scholar: [Author Only](#) [Title Only](#) [Author and Title](#)

**Gisbert C, Rus AM, Bolarin MC, Lopez–Coronado JM, Arrillaga I, Montesinos C, Caro M, Serrano R, Moreno V (2000) The yeast HAL1 gene improves salt tolerance of transgenic tomato. *Plant Physiol* 123: 392–402**

Pubmed: [Author and Title](#)

CrossRef: [Author and Title](#)

Google Scholar: [Author Only](#) [Title Only](#) [Author and Title](#)

**Gleave AP (1992) A versatile binary vector system with a T-DNA organisational structure conducive to efficient integration of cloned DNA into the plant genome. *Plant Mol Biol* 20: 1203–1207**

Pubmed: [Author and Title](#)

CrossRef: [Author and Title](#)

Google Scholar: [Author Only](#) [Title Only](#) [Author and Title](#)

**Hasegawa PM (2013) Sodium (Na<sup>+</sup>) homeostasis and salt tolerance of plants. *Environ Exp Bot* 92: 19–31**

Pubmed: [Author and Title](#)

CrossRef: [Author and Title](#)

Google Scholar: [Author Only](#) [Title Only](#) [Author and Title](#)

**Hedrich R, Marten I (2011) TPC1 – SV Channels Gain Shape. *Mol Plant* 4: 428-441**

Pubmed: [Author and Title](#)

CrossRef: [Author and Title](#)

Google Scholar: [Author Only](#) [Title Only](#) [Author and Title](#)

**Hirschi K.D (1999) Expression of Arabidopsis CAX1 in Tobacco: Altered calcium homeostasis and increased stress sensitivity. *Plant Cell* 11: 2113-2122**

Pubmed: [Author and Title](#)

CrossRef: [Author and Title](#)

Google Scholar: [Author Only](#) [Title Only](#) [Author and Title](#)

**Hoagland DR Arnon DI (1950) The water–culture method for growing plants without soil. In: *Agricultural Experiment Station Circular 347, Berkeley, The College of Agriculture University of California*, 1–32**

Pubmed: [Author and Title](#)

CrossRef: [Author and Title](#)

Google Scholar: [Author Only](#) [Title Only](#) [Author and Title](#)

**Huertas R, Rubio L, Cagnac O, García-Sánchez MJ, Alché JDD, Venema K, Fernández JA, Rodríguez–Rosales MP (2013) The K<sup>+</sup>/H<sup>+</sup> antiporter LeNHX2 increases salt tolerance by improving K<sup>+</sup> homeostasis in transgenic tomato. *Plant Cell Environ* 36: 2135-2149**

Pubmed: [Author and Title](#)

CrossRef: [Author and Title](#)

Google Scholar: [Author Only](#) [Title Only](#) [Author and Title](#)

**Kang HK, Nam KH (2016) Reverse function of ROS-induced CBL10 during salt and drought stress responses. *Plant Sci* 243: 49-55**

Pubmed: [Author and Title](#)

CrossRef: [Author and Title](#)

Google Scholar: [Author Only](#) [Title Only](#) [Author and Title](#)

**Kim BG, Waadt R, Cheong YH, Pandey GK, Dominguez-Solis JR, Schültke S, Lee SC, Kudla J, Luan S (2007) The calcium sensor CBL10 mediates salt tolerance by regulating ion homeostasis in Arabidopsis. *Plant J* 52: 473-484**

Pubmed: [Author and Title](#)

CrossRef: [Author and Title](#)

Google Scholar: [Author Only](#) [Title Only](#) [Author and Title](#)

**Kim KN (2013) Stress responses mediated by the CBL calcium sensors in plants. *Plant Biotechnol Rep* 7: 1-8**

Pubmed: [Author and Title](#)

CrossRef: [Author and Title](#)

Google Scholar: [Author Only](#) [Title Only](#) [Author and Title](#)

**Kintzer AF, Stroud RM (2016) Structure, inhibition and regulation of two-pore channel TPC1 from Arabidopsis thaliana. *Nature* 531: 258-264.**

Pubmed: [Author and Title](#)  
CrossRef: [Author and Title](#)  
Google Scholar: [Author Only](#) [Title Only](#) [Author and Title](#)

**Kolukisaoglu Ü, Weini S, Blazevic D, Batistic O, Kudla J (2004) Calcium sensors and their interacting protein kinases: genomics of the Arabidopsis and rice CBL-CIPK signaling networks. Plant Physiol 134: 43-58**

Pubmed: [Author and Title](#)  
CrossRef: [Author and Title](#)  
Google Scholar: [Author Only](#) [Title Only](#) [Author and Title](#)

**Lin H, Yang Y, Quan R, Mendoza I, Wu Y, Du W, Zhao S, Schumaker KS, Pardo JM, Guo Y (2009) Phosphorylation of SOS3-like calcium binding protein 8 by SOS2 protein kinase stabilizes their protein complex and regulates salt tolerance in Arabidopsis. Plant Cell 21: 1607-1619**

Pubmed: [Author and Title](#)  
CrossRef: [Author and Title](#)  
Google Scholar: [Author Only](#) [Title Only](#) [Author and Title](#)

**Livak KJ, Schmittgen TD (2001) Analysis of relative gene expression data using real-time quantitative PCR and the 2(-Delta Delta C(T)) method. Methods 25: 402-408**

Pubmed: [Author and Title](#)  
CrossRef: [Author and Title](#)  
Google Scholar: [Author Only](#) [Title Only](#) [Author and Title](#)

**Luan S (2008) The CBL-CIPK network in plant calcium signaling. Trends Plant Sci 14: 37-42**

Pubmed: [Author and Title](#)  
CrossRef: [Author and Title](#)  
Google Scholar: [Author Only](#) [Title Only](#) [Author and Title](#)

**Maathuis FJM (2009) Physiological functions of mineral macronutrients. Curr Opin Plant Biol 12: 250-258**

Pubmed: [Author and Title](#)  
CrossRef: [Author and Title](#)  
Google Scholar: [Author Only](#) [Title Only](#) [Author and Title](#)

**Maathuis FJM (2014) Sodium in plants: perception, signalling, and regulation of sodium fluxes. J Exp Bot 65: 849-858**

Pubmed: [Author and Title](#)  
CrossRef: [Author and Title](#)  
Google Scholar: [Author Only](#) [Title Only](#) [Author and Title](#)

**Maeshima M (2000) Vacuolar H<sup>+</sup>-pyrophosphatase. Biochim Biophys Acta 1465: 37-51**

Pubmed: [Author and Title](#)  
CrossRef: [Author and Title](#)  
Google Scholar: [Author Only](#) [Title Only](#) [Author and Title](#)

**Manaa A, Faurobert M, Valot B, Bouchet JP, Grasselly D, Causse M, Ahmed HB (2013) Effect of salinity and calcium on tomato fruit proteome. OMICS 17:328-352**

Pubmed: [Author and Title](#)  
CrossRef: [Author and Title](#)  
Google Scholar: [Author Only](#) [Title Only](#) [Author and Title](#)

**Manohar M, Shigaki T, Hirschi KD (2011) Plant cation/H<sup>+</sup> exchangers (CAxS): biological functions and genetic manipulation. Plant Biol 13: 561-569**

Pubmed: [Author and Title](#)  
CrossRef: [Author and Title](#)  
Google Scholar: [Author Only](#) [Title Only](#) [Author and Title](#)

**Monihan SM, Magness CA, Yadegari R, Smith SE, Schumaker KS (2016) Arabidopsis CALCINEURIN B-LIKE10 functions independently of the SOS pathway during reproductive development in saline conditions. Plant Physiol 171: 369-379**

Pubmed: [Author and Title](#)  
CrossRef: [Author and Title](#)  
Google Scholar: [Author Only](#) [Title Only](#) [Author and Title](#)

**Murashige T, Skoog F (1962) A revised medium for rapid growth and bio assays with Tobacco tissue cultures. Physiol Plant 15: 473-497**

Pubmed: [Author and Title](#)  
CrossRef: [Author and Title](#)  
Google Scholar: [Author Only](#) [Title Only](#) [Author and Title](#)

**Olias R, Eljakaoui Z, Li J, de Morales PA, Marin-Manzano MC, Pardo JM, Belder A (2009) The plasma membrane Na<sup>+</sup>/H<sup>+</sup> antiporter SOS1 is essential for salt tolerance in tomato and affects the partitioning of Na<sup>+</sup> between plant organs. Plant Cell Environ 32: 904-916**

Pubmed: [Author and Title](#)  
CrossRef: [Author and Title](#)  
Google Scholar: [Author Only](#) [Title Only](#) [Author and Title](#)

**Park S, Cheng NH, Pittman JK, Yoo KS, Park J, Smith RH, Hirschi KD (2005) Increased calcium levels and prolonged shelf life in tomatoes expressing Arabidopsis H<sup>+</sup>/Ca<sup>2+</sup> transporters. Plant Physiol 139: 1194-206**

Pubmed: [Author and Title](#)  
CrossRef: [Author and Title](#)

Google Scholar: [Author Only](#) [Title Only](#) [Author and Title](#)

**Peiter E (2011) The plant vacuole: Emitter and receiver of calcium signals. Cell Calcium 50: 120-128**

Pubmed: [Author and Title](#)

CrossRef: [Author and Title](#)

Google Scholar: [Author Only](#) [Title Only](#) [Author and Title](#)

**Pérez-Martín F, Yuste-Lisbona FJ, Pineda B, Angarita-Díaz MP, García-Sogo B, Antón T, Sánchez S, Giménez E, Atarés A, Fernández-Lozano A, et al (2017) A collection of enhancer trap insertional mutants for functional genomics in tomato. Plant Biotechnol J 15:1439-1452**

Pubmed: [Author and Title](#)

CrossRef: [Author and Title](#)

Google Scholar: [Author Only](#) [Title Only](#) [Author and Title](#)

**Pineda B, García-Abellán JO, Antón T, Pérez F, Moyano E, García-Sogo B, Campos JF, Angosto T, Morales B, Capel J, et al. (2012) Genomic approaches for salt and drought stress tolerance in tomato. In N Tuteja, SS Gill, AF Tiburcio, R Tuteja, eds, Improving Crop Resistance to Abiotic Stress. Wiley-VCH Verlag and Co. KGaA, Weinheim. 1085–1110**

Pubmed: [Author and Title](#)

CrossRef: [Author and Title](#)

Google Scholar: [Author Only](#) [Title Only](#) [Author and Title](#)

**Pittman JK, Edmond C, Sunderland PA, Bray CM (2009) A cation-regulated and proton gradient-dependent cation transporter from *Chlamydomonas reinhardtii* has a role in calcium and sodium homeostasis. J Biol Chem 284: 525-533**

Pubmed: [Author and Title](#)

CrossRef: [Author and Title](#)

Google Scholar: [Author Only](#) [Title Only](#) [Author and Title](#)

**Platten JD, Cotsaftis O, Berthomieu P, Bohnert H, Davenport RJ, Fairbairn DJ, Horie T, Leigh RA, Lin HX, Luan S, et al. (2006) Nomenclature for HKT transporters, key determinants of plant salinity tolerance. Trends Plant Sci 11: 372–374**

Pubmed: [Author and Title](#)

CrossRef: [Author and Title](#)

Google Scholar: [Author Only](#) [Title Only](#) [Author and Title](#)

**Qiu QS, Guo Y, Quintero FJ, Pardo JM, Schumaker KS, Zhu JK (2004) Regulation of vacuolar Na<sup>+</sup>/H<sup>+</sup> exchange in *Arabidopsis thaliana* by the salt-overly-sensitive (SOS) pathway. J Biol Chem 279: 207–15**

Pubmed: [Author and Title](#)

CrossRef: [Author and Title](#)

Google Scholar: [Author Only](#) [Title Only](#) [Author and Title](#)

**Quan R, Lin H, Mendoza I, Zhang Y, Cao W, Yang Y, Shang M, Chen S, Pardo JM, Guo Y (2007) SCABP8/CBL10, a putative calcium sensor, interacts with the protein kinase SOS2 to protect *Arabidopsis* shoots from salt stress. Plant Cell 19: 1415–31**

Pubmed: [Author and Title](#)

CrossRef: [Author and Title](#)

Google Scholar: [Author Only](#) [Title Only](#) [Author and Title](#)

**Robertson D (2013) Modulating Plant Calcium for Better Nutrition and Stress Tolerance. ISRN Botany Article ID 952043.**

Pubmed: [Author and Title](#)

CrossRef: [Author and Title](#)

Google Scholar: [Author Only](#) [Title Only](#) [Author and Title](#)

**Shabala S (2013) Learning from halophytes: physiological basis and strategies to improve abiotic stress tolerance in crops. Ann Bot 112: 1209–1221**

Pubmed: [Author and Title](#)

CrossRef: [Author and Title](#)

Google Scholar: [Author Only](#) [Title Only](#) [Author and Title](#)

**Shabala S, Shabala L, Van Volkenburgh E, Newman I (2005) Effect of divalent cations on ion fluxes and leaf photochemistry in salinized barley leaves. J Exp Bot 56: 1369–78**

Pubmed: [Author and Title](#)

CrossRef: [Author and Title](#)

Google Scholar: [Author Only](#) [Title Only](#) [Author and Title](#)

**Tang RJ, Yang Y, Yang L, Liu H, Wang CT, Yu MM, Gao XS, Zhang HX (2014) Poplar calcineurin B-like proteins PtCBL10A and PtCBL10B regulate shoot salt tolerance through interaction with PtSOS2 in the vacuolar membrane. Plant Cell Environ 37: 573–88**

Pubmed: [Author and Title](#)

CrossRef: [Author and Title](#)

Google Scholar: [Author Only](#) [Title Only](#) [Author and Title](#)

**Uozumi A, Ikeda H, Hiraga M, Kanno H, Nanzyo M, Nishiyama M, Kanayama Y (2012) Tolerance to salt stress and blossom-end rot in an introgression line, IL8-3, of tomato. Sci Hortic 138: 1-6**

Pubmed: [Author and Title](#)

CrossRef: [Author and Title](#)

Google Scholar: [Author Only](#) [Title Only](#) [Author and Title](#)

**Villalta I, Reina-Sánchez A, Bolarín MC, Cuartero J, Belver A, Venema K, Carbonell EA, Asins MJ (2008) Genetic analysis of Na<sup>+</sup> and K<sup>+</sup>**

**concentrations in leaf and stem as physiological components of salt tolerance in Tomato. Theor Appl Genet 116: 869-80**

Pubmed: [Author and Title](#)

CrossRef: [Author and Title](#)

Google Scholar: [Author Only](#) [Title Only](#) [Author and Title](#)

**Waadt R, Schmidt LK, Lohse M, Hashimoto K, Bock R, Kudla J (2008) Multicolor bimolecular fluorescence complementation reveals simultaneous formation of alternative CBL/CIPK complexes in planta. Plant J 56: 505–16**

Pubmed: [Author and Title](#)

CrossRef: [Author and Title](#)

Google Scholar: [Author Only](#) [Title Only](#) [Author and Title](#)

**Wesley SV, Helliwell CA, Smith NA, Wang M, Rouse DT, Liu Q, Gooding PS, Singh SP, Abbott D, Stoutjesdijk PA, et al. (2001) Construct design for efficient, effective and high-throughput gene silencing in plants. Plant J 27: 581–590**

Pubmed: [Author and Title](#)

CrossRef: [Author and Title](#)

Google Scholar: [Author Only](#) [Title Only](#) [Author and Title](#)

**White PJ, Broadley MR (2003) Calcium in plants. Ann Bot–Lond 92: 487–511**

Pubmed: [Author and Title](#)

CrossRef: [Author and Title](#)

Google Scholar: [Author Only](#) [Title Only](#) [Author and Title](#)

**Yuste–Lisbona FJ, Quinet M, Fernández–Lozano A, Pineda B, Moreno V, Angosto T, Lozano R (2016) Characterization of vegetative inflorescence (mc–vin) mutant provides new insight into the role of MACROCALYX in regulating inflorescence development of tomato. Sci Reps 6: 18796**

Pubmed: [Author and Title](#)

CrossRef: [Author and Title](#)

Google Scholar: [Author Only](#) [Title Only](#) [Author and Title](#)

**Zhai Y, Yang Q, Hou M (2015) The effects of saline water drip irrigation on tomato yield, quality, and blossom–end rot incidence – A 3a Case study in the South of China. PLoS One 10: e0142204**

Pubmed: [Author and Title](#)

CrossRef: [Author and Title](#)

Google Scholar: [Author Only](#) [Title Only](#) [Author and Title](#)